Mechanisms of Microwave Induced
Damage in Biologic Materials

DTIC
ELECTE
FEB 0 8 1990
D

Annual Report

January, 1989

EFFECTS OF ELECTROMAGNETIC FIELDS
ON BIOLOGICAL MATERIALS AND PROCESSES

by

T. A. Litovitz, Robert Meister, Robert K. Mohr,
C. J. Montrose, J. Michael Mullins, Roland M. Nardone
Miguel Penafiel and Constantino Grosse

Contract DAMD17-86-C-6260

The Catholic University of America
Washington, DC 20064

90 02 07 055

REPORT DOCUMENTATION PAGE

1a. REPORT SECURITY CLASSIFICATION Unclassified		1b. RESTRICTIVE MARKINGS			
2a. SECURITY CLASSIFICATION AUTHORITY		3. DISTRIBUTION/AVAILABILITY OF REPORT Distribution for public release; distribution unlimited			
2b. DECLASSIFICATION/DOWNGRADING SCHEDULE					
4. PERFORMING ORGANIZATION REPORT NUMBER(S)		5. MONITORING ORGANIZATION REPORT NUMBER(S)			
6a. NAME OF PERFORMING ORGANIZATION The Catholic University of America	6b. OFFICE SYMBOL (If applicable)	7a. NAME OF MONITORING ORGANIZATION			
6c. ADDRESS (City, State, and ZIP Code) Washington, DC 20064		7b. ADDRESS (City, State, and ZIP Code)			
8a. NAME OF FUNDING/SPONSORING ORGANIZATION US Army Medical Research & Development Command	8b. OFFICE SYMBOL (If applicable)	9. PROCUREMENT INSTRUMENT IDENTIFICATION NUMBER DAMD17-86- C-6260			
8c. ADDRESS (City, State, and ZIP Code) Fort Detrick Frederick, Maryland 21701-5012		10. SOURCE OF FUNDING NUMBERS			

10. SOURCE OF FUNDING NUMBERS			
PROGRAM ELEMENT NO.	PROJECT NO.	TASK NO.	WORK UNIT ACCESSION NO.
62777A	62777A878	BB	021

11. TITLE (Include Security Classification)

(U) Mechanisms of Microwave Induced Damage in Biologic Materials

12. PERSONAL AUTHOR(S)

13a. TYPE OF REPORT Annual Report	13b. TIME COVERED FROM 9/22/87 TO 9/21/88	14. DATE OF REPORT (Year, Month, Day) 1989 January	15. PAGE COUNT 75

16. SUPPLEMENTARY NOTATION
Subtitle: Effects of Electromagnetic Fields on Biological Materials and Processes

17. COSATI CODES			18. SUBJECT TERMS (Continue on reverse if necessary and identify by block number)
FIELD	GROUP	SUB-GROUP	RA 3; Microwave; Irradiation; Cell cultures; Deoxyribonucleic acid (EMF)
06	03		
06	01		

19. ABSTRACT (Continue on reverse if necessary and identify by block number)
This research program to elucidate the athermal effects of electromagnetic fields and biological systems has divided along two main focus areas: one involving a primarily physical approach to the problem, the second involving a biological approach. The physical approach has taken the form of (1) dynamical modeling studies that attempt to characterize the interaction mechanism and explore some of its consequences, and (2) microwave, dielectric and optical spectroscopic studies in which the interactions of high frequency fields with DNA molecules are studied. The modeling work included both molecular dynamics simulation studies and phenomenological lines of attack. In the latter, a "depletion model" has been developed which accounts semiquantitatively for may of the observed features of gene expression alteration by electromagnetic fields. The spectroscopic work--particularly the dielectric relaxation studies--has yielded significant insights into the dynamics of molecular, ionic, and cellular responses to exogenous fields.

The biological attack on the problem has examined the response of various cell cultures to

20. DISTRIBUTION/AVAILABILITY OF ABSTRACT ☐ UNCLASSIFIED/UNLIMITED ☐ SAME AS RPT. ☐ DTIC USERS	21. ABSTRACT SECURITY CLASSIFICATION
22a. NAME OF RESPONSIBLE INDIVIDUAL	22b. TELEPHONE (Include Area Code) 22c. OFFICE SYMBOL

DD Form 1473, JUN 86   Previous editions are obsolete.   SECURITY CLASSIFICATION OF THIS PAGE

19. microwave exposures of varying durations. A number of endpoints including cell growth, viability, plating efficiency, membrane related differentiation functions and cell cycle progression were found not to be altered by continuous--wave, sinusoidal--or pulse-modulated microwave exposures. Two specific enqume systems were selected for analysis and a two dimensional gel electrophoresis system was developed so that both particular and general endpoints were studied. Of the two enzyme systems, the interferon related system (RNase L and 2-5A synthetase activities) showed enhanced activities to microwave exposure. The other, ornithine decarboxylase, showed no response to continuous wave exposure; studies involving modulate microwaves are continuing.

FOREWORD

Citations of commercial organizations and trade names in this report do not constitute an official Department of the Army endorsement or approval of the products or services of these organizations.

Accesion For	
NTIS CRA&I	☑
DTIC TAB	☐
Unannounced	☐
Justification	
By	
Distribution /	
Availability Codes	
Dist	Avail and / or Special
A-1	

TABLE OF CONTENTS

I.   PHYSICAL APPROACH TO THE PROBLEM

There exists a wealth of experimental evidence establishing the proposition that irradiation with electromagnetic (EM) fields affects gene expression. The research described here represents the main features of a program designed to develop an understanding of this at two levels:

(1)   Phenomenologically we have developed what we term a "depletion model" to account for the gross features of the dynamical effect of EM fields; and

(2)   At a molecular level we have designed and are performing a set of experiments aimed at elucidating the physical character of the interaction mechanisms by which EM energy is coupled into DNA molecules.

In the paragraphs that follow we report on the accomplishments and progress in these two areas. We consider first the dynamical modeling efforts and then describe the spectroscopic work than that has been and is being carried out. We also describe the design and engineering of new systems for achieving desired irradiation conditions of biological systems.

1.   Dynamical Modeling

A.   The Depletion Model

A number of experimenters (ourselves included) have reported that the exposure of cells to relatively low intensity pulsed and low frequency electromagnetic fields results in a transient augmentation of transcriptional activity. Surprisingly the increases have been seen under certain irradiation conditions to exhibit maxima when regarded as a function of the strength of the electromagnetic fields. We have developed a simple multi-step chemical reaction model that accounts for the principal features that are observed both in the time and power variation of the transcriptional effects. The crucial hypothesis of the model is the supposition that the direct effect of cell exposure to electromagnetic fields is an increase in the rate constant characterizing one of the sequential reactions in the synthesis of mRNA.

We assume that the synthesis of messenger RNA and the subsequent protein production can be schematically represented by a set of sequential reactions as

$$A \xrightarrow{\quad k_1 \quad} X \xrightarrow{\quad k_2 \quad} Y \xrightarrow{\quad k_3 \quad} Z$$

3
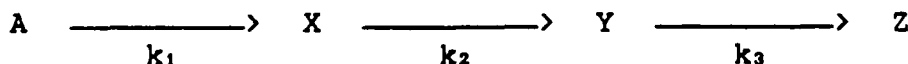
Where, for example, A represents the nucleotide pool in the cell, and the process $A \rightarrow X$ is the diffusion controlled migration of these nucleotides to the neighborhood of the DNA. The other steps in the symbolic reaction scheme represent the transcription process (resulting in the production of messenger RNA, denoted by Y), and the translation process (producing proteins, Z). The k's are the effective rate constants for the various steps.

We designate the concentrations of the various products by x, y and z respectively and write first order differential equations governing their production:

$$dx/dt = k_1 A - k_2 x \qquad (1a)$$

$$dy/dy = k_2 x - k_3 y \qquad (1b)$$

etc.

We have assumed that the nucleotide pool A constitute a reservoir that is rapidly replenished, and also that the back reactions, e.g., $Y \rightarrow X$, can be ignored. The steady-state situation, is described by $dx/dt = dy/dt = \cdots = 0$ and $x = x_0$, $y = y_0$, ... , from which we can obtain

$$x_0 = k_1 A/k_2 \qquad \text{and} \qquad y_0 = k_2 x_0/k_3 = k_1 A/k_3 . \qquad (2)$$

Suppose now that at some instant, say at time $= 0$ (when steady-state conditions are extant), the system is subjected to electromagnetic irradiation.

We assume that the effect of the electromagnetic field is to alter the rate constant k_2, increasing it to some new value $k_2{}^*$.

For $t>0$, the concentrations x, y, z, ... are time dependent. It is a straightforward matter to solve the differential equations to obtain the results:

$$x(t) = \frac{k_1 A}{k_2{}^*} \left[1 + \left(\frac{\Delta k}{k_2}\right) e^{-k_2{}^* t} \right] \qquad (3a)$$

and

$$y(t) = \frac{k_1 A}{k_3} + \frac{k_1 A}{k_3 - k_2{}^*} \left(\frac{\Delta k}{k_2}\right) \left[e^{-k_2{}^* t} - e^{-k_3 t} \right] \qquad (3b)$$

where $\Delta k = k_2{}^* - k_2$.

These two equations are two of the important conclusions of the model. Observe from Eq. (3a) that x, the concentration of nucleotides near the DNA, decreases from its zero-field value of

4

$k_1 A/k_2$ to its steady state value $k_1 A/k_2^*$ as a result of the increased transcription rate. The concentration of messenger RNA, $x(t)$, first rises as a result of the enhancement of the rate k_2, but then decays eventually to its basal value as a result of the depletion of the nucleotides. The excess mRNA activity above the basal value, that is, $y(t) - y_0$ is is plotted in Figure 1 for several values of the parameter $\Delta k/k_2$ (the values for the other parameters are given in Table 1). We assume that $\Delta k/k_2$ increases as the irradiating field strength is increased.

TABLE 1. Parameters used in constructing Figs. 1-5.		
	Figs. 1-3	Figs. 4-5
A (arbitrary units)	10	10
k_1 (min^{-1})	1.0	1.0
k_2 (min^{-1})	0.001	0.01
k_2^* (min^{-1})	0.008 0.040 0.100	0.1
k_3 (min^{-1})	0.800	0.2

Observe in Fig. 1 that for an irradiation time of 20 minutes the response (i.e., y, the mRNA concentration) is largest for the intermediate exposure conditions. If the only "data" that were presented were these 30-minute exposure results considered as a function of irradiating field strength (see Fig. 2), then it would be quite natural to infer that the biological system exhibits an enhanced sensitivity to fields near the intermediate value. As is evident, however, such a conclusion would make little sense in view of the time evolution of the response as shown in Fig. 1. It is tempting to speculate that many of the so-called "power windows" that have been reported in the literature might be explained in a fashion similar to this.

Observe that even under the assumption that $\Delta k \propto E$, there are no obvious features in the response curves of Fig. 1 which are linearly related to the field strength (the height of the peak, for instance does not quintuple in going from the intermediate to the largest field strength). However, by differentiating Eq. (3b) we can obtain the result

$$\frac{dy}{dt}\bigg|_{t=0} = \frac{k_1 A}{k_2} \Delta k$$

5

which indicates that the initial slope of the response curves in Fig. 1 is directly proportional to Δk, and thus (by assumption) to the electric field strength. This behavior is evident in Fig. 3 in which the early region of Fig. 1 is shown in detail.

We may also ask about how the system responds when the field is switched off. If we hypothesize that the immediate effect of this is to cause the return of the rate constant to its original value, i.e., $k_2^* \rightarrow k_2$, then we can obtain the desired results simply by resolving the differential equation subject to the appropriate initial conditions. Assume that following the initial imposition of the field, sufficient time passed to allow both x and y to reach their steady state values. At this instant, say time = t*, the field is suddenly switched off. The time dependence of x and y for t≥t* is then given by

$$x(t) = \frac{k_1 A}{k_2} [1 - (\frac{\Delta k}{k_2^*}) e^{-k_2 \Delta t}] \tag{4a}$$

and

$$y(t) = \frac{k_1 A}{k_3} - \frac{k_1 A}{k_3 - k_2} (\frac{\Delta k}{k_2^*}) [e^{-k_2 \Delta t} - e^{-k_3 \Delta t}] \tag{4b}$$

where $\Delta t = t - t^*$. The complete time dependence of the mRNA concentration is plotted in Fig. 4. Note particularly that the mRNA concentration dips below its steady-state basal value following the removal of the radiation field, reaches a minimum value, and ultimately returns to its basal value as $t \rightarrow \infty$. This "rebound" effect has not as yet been reported in the literature. We have initiated efforts (now under way) to observe this behavior.

One last point should be discussed. We suppose that the proteins produced (Z in the reaction chain) in the translation process are relatively long-lived, in the sense that, their own denaturing proceeds much more slowly than all other relevant dynamical steps. Then it is a fairly simple matter to obtain the protein concentration z(t) from dz/dt = k_3 y as

$$z(t) = k_3 \int_0^t dt' \, y(t');$$

$$z(t) = k_1 A t + \frac{k_1 A}{k_3 - k_2^*} (\frac{\Delta k}{k_2^*}) [\frac{k_3}{k_2^*}(1 - e^{-k_2^* t}) - (1 - e^{-k_3 t})]. \tag{5}$$

The linearly increasing first term which describes the normal production of protein in the absence of external irradiation. If we focus on the second term (call it δz) which describes the effect of the irradiation, it is clear that this term initially

rises quadratically, reaches an inflection point, and ultimately levels off at a limiting value of

$$\delta z(t \rightarrow \infty) \equiv \delta z_\infty = k_1 A \left(\frac{1}{k_2} - \frac{1}{k_2^*}\right).$$

Observe that for $k_2^* \gg k_2$, this becomes $\delta z_\infty \approx k_1 A/k_2$; the limiting value is independent of the strength of the irradiating field, i.e., of the change in k_2. The variation of δz is shown in Fig. 5. This result means that one cannot linearly extrapolate large dose observations to lower doses (as is often done) to establish "safe" exposure levels. The dependence of the response (δz) on the field strength is just much too complicated for a naive linear extrapolation to be meaningful.
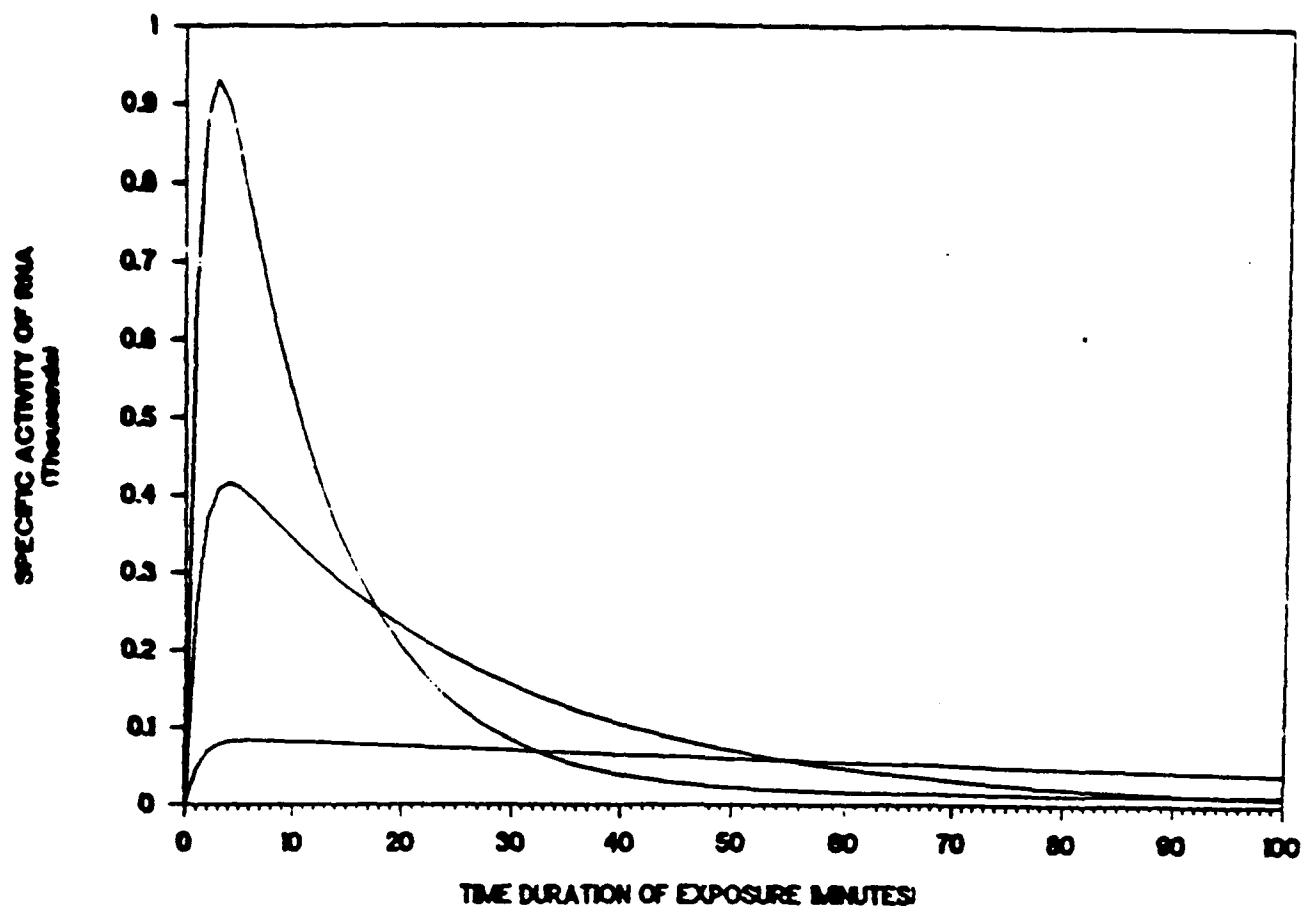
7

EFFECT OF EM FIELDS ON RNA SYNTHESIS

Figure 1. Excess mRNA activity plotted as a function of time [y(t) vs. t] following the switching on of an incident electromagnetic field computed from Eq. (3b). The parameters used are given in Table 1, with the curve with the highest peak corresponding to the largest value of k_2 .

8

Figure 2. Levels of mRNA following 30-minute exposure to three different electromagnetic field strengths. The three situations correspond respectively, to changes in k_2 from 0.001 min^{-1} to 0.008, 0.040 and 0.100 min^{-1}.

EFFECT OF EM FIELDS ON RNA SYNTHESIS
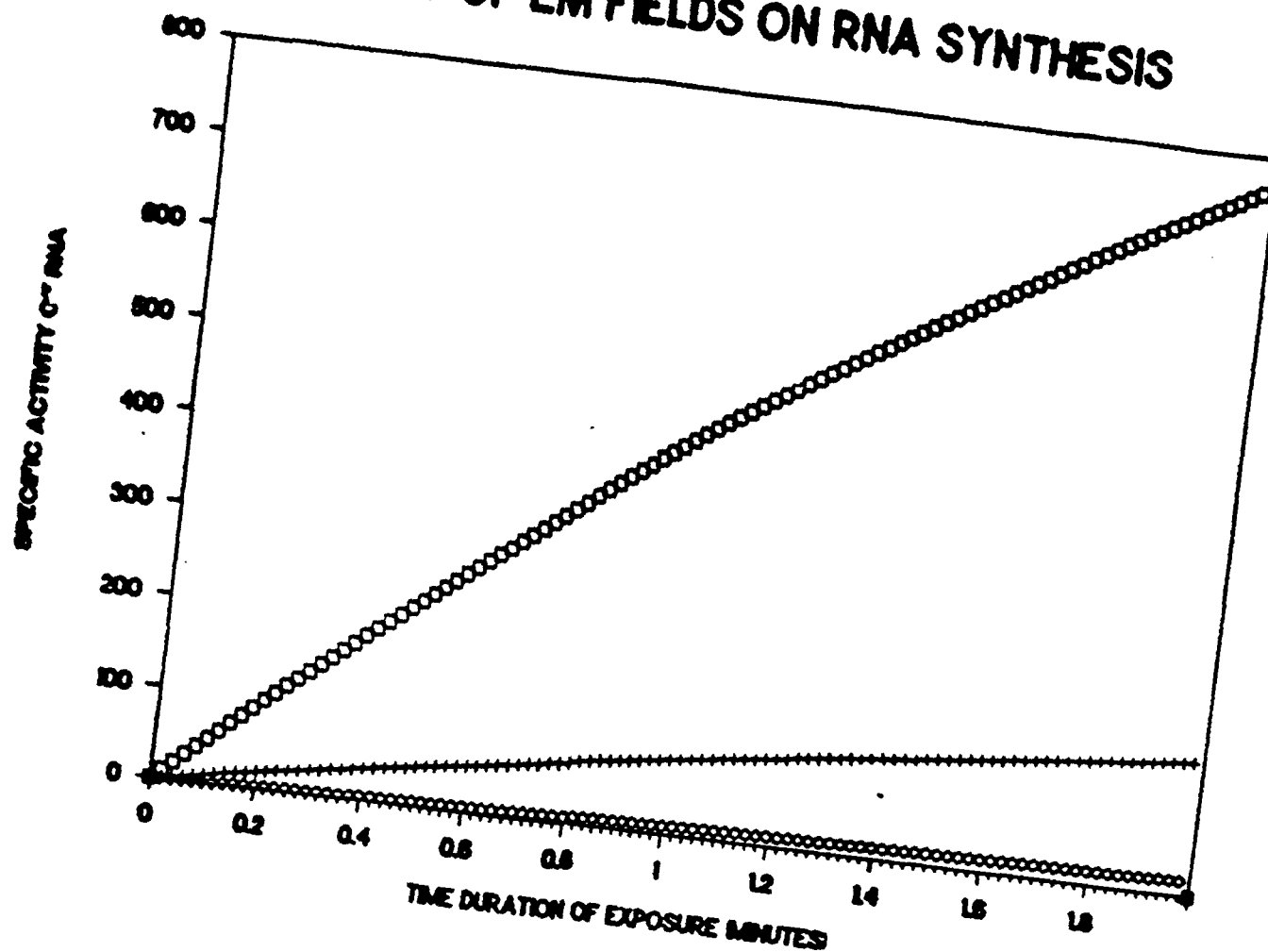
Figure 3. The same data as in Figure 1 but with the short time portion of the response expanded. The largest change in k_2 leads to the most rapid increase.

10

EFFECT OF EM FIELDS ON RNA SYNTHESIS

EXPOSURE TIME 100 MINUTES
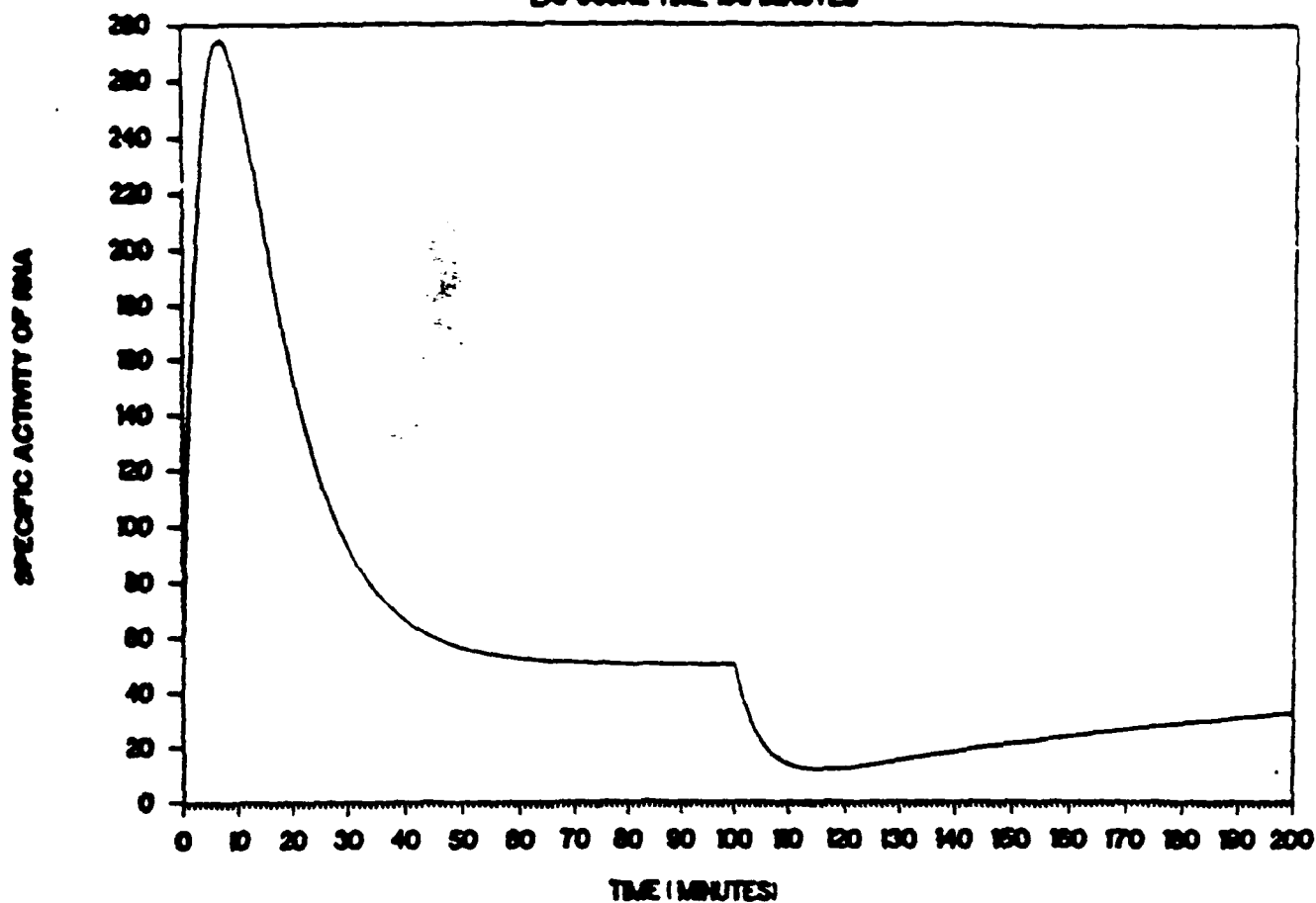
Figure 4.   The response of the system (mRNA levels) as a function of time for an irradiation schedule in which the field is switched on at time = 0 and switched off at time = 100 minutes.

EXCESS PROTEIN PRODUCED

Figure 5.   The dependence of the excess protein production δz_∞ as a function of field strength.   The curve is computed from Equation (6) under the assumption that $\Delta k \propto E$.

12

B.   Molecular Dynamics

The molecular dynamics computer simulation studies were designed to provide some insight about a number of features of polyelectrolyte solutions. These include the following:

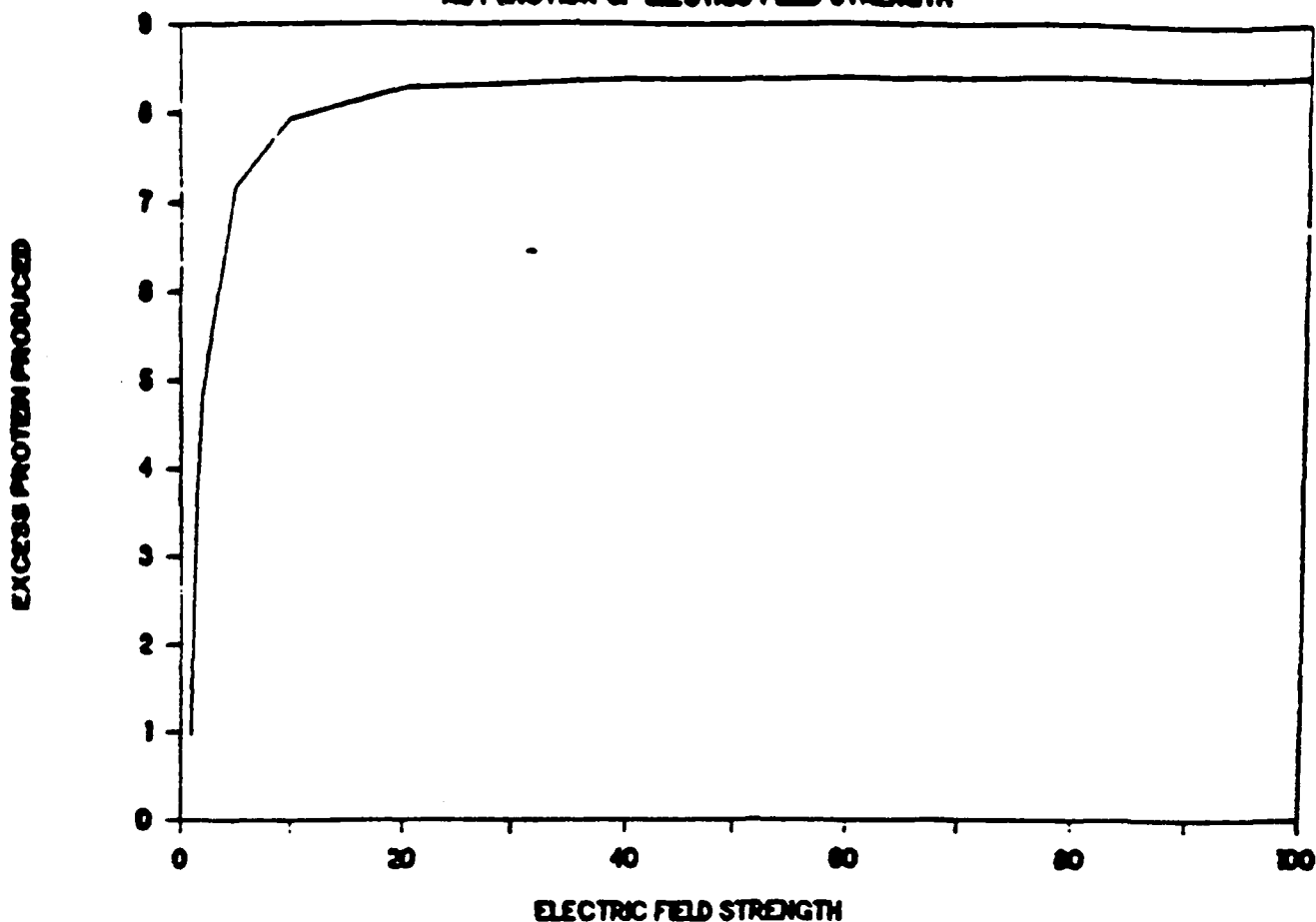(1)   We have considered the energy transfer processes that occur in the interaction between a charged polymeric molecule in an electrolytic solvent and a suddenly impressed electric field. In particular, we have attempted to examine the non-resonant excitation of internal vibrations of the polymer, resulting from collisions with ions set into motion by externally impressed fields.

(2)   We have attempted to understand the distribution (clustering) of counter-ions and co-ions around a single electrically charged polymer molecule in solution, both in the presence and in the absence of externally applied electric fields. We have examined the time-dependent response of the ionic distribution to the switching on of the field.

The model system under examination was composed of 1000 atoms, six of which were harmonically bound to form a linear molecule. These six atoms were each given a negative electric charge. The molecule is immersed in a liquid solvent of 994 atoms of which 50 are positively charged and a number are negatively charged, that number being chosen to ensure charge neutrality of the system (it was a variable as various values were examined for the charge on each polymer atom). All atoms in the system interacted with one another via Lennard-Jones 6-12 forces, as well as the appropriate electrical forces for the charged particles. At various times in the modeling, one or more of these electrical forces were turned off in an effort to understand the individual effects of the various interactions.

In the early studies, no restrictions were placed on the angle between adjacent bonds in the polymer molecule. The individual atoms thus enjoyed extraordinary freedom of movement. In the presence of the positively charged counter ions, the molecule tended to wrap itself rather tightly around one of the ions, and then to attract a roughly spherical sheath of additional positively charged ions around it. In this configuration the polymer was quite effectively shielded from further interactions with moving ions, the whole assembly simply moving electrophoretically in the impressed field.

To stiffen the polymer backbone so that the polymer will couple more effectively to ionic motions in the surrounding media, we added a set of constraining forces to the molecule such that the angle between adjacent bonds is maintained. This

13

accelerated the exchange of energy between the internal vibrations of the polymer molecule and the field-induced dynamics of the surrounding medium.

For this system, we obtained the surprising observation that for field strengths of 2 and 4 (in reduced LJ units) the energy associated with internal vibrations *decreases* when the field is switched on, indicating a coupling of energy from these vibrations to the molecule's ionic environment. That is, energy is transferred out of the molecular vibrations into the energy reservoir of the fluid as a whole. While this leads to the possibility of athermal non-resonant absorption of energy by the system as a whole, it does not imply excitation of the electrically charged polymer molecules.

When the MD experiment was repeated from a different initial configuration, but under the same temperature, pressure and density conditions, essentially the same generic result was obtained. That is again the energy was observed to couple out of the vibrational degrees of freedom of the molecule and into the translational energy of the solvent. Though there were some quantitative differences in the runs, the qualitative conclusions were unchanged.

In addition MD experiments in solutions in which no external temperature control is imposed were made. In contrast with the earlier results which were obtained under quasi-isothermal conditions, i.e., at each time-step in the computation, the velocities of the solvent molecules and ions were scaled to maintain their total kinetic energy as a constant. In the MD experiments reported here, the polymers in solution were made rather rigid with only internal vibrational modes being allowed. It was felt that this would accelerate energy transfers between the molecule and its environment, an important consideration, since significant temperature rises are expected to occur, and once this occurs, interpretation of the results is difficult.

Immediately after switching on the field the results in terms of energy coupling were essentially as before--a slow transfer of energy out of the molecular degrees of freedom into the fluid as a whole was observed. As before the switching on of the field effected a tighter packing of counter ions around the polyions, but, since these molecules are in this study quite rigid, no significant changes in their structure occurred. At somewhat longer times after the field was turned on the temperature of the system rose significantly and eventual coupling of energy into the intra-molecular vibrations was observed.

14

2. Spectroscopic Studies

A. Coupling of Microwave Energy into the Environment of DNA Molecules

Experimental results[1-17] have shown that the dielectric spectra of polyelectrolyte solutions display several dispersion regions corresponding to different mechanisms of polarization relaxation. In various theoretical approaches, such phenomena as electrode polarization, fluctuations in the distribution of counterions, restricted motion of "bound" water molecules, among others have been considered as candidates to explain the observed relaxation processes. In the paragraphs that follow, we review some of these mechanisms to provide context and background for the results and their interpretation that are reported.

Theory of counterion condensation

Most of the models that have been advanced are independent of developments in the theory of polyelectrolytes, the fundamentals of which were proposed by Manning[16,17]. Of primary importance in this treatment is the phenomenon of counterion condensation, which, together with ionic screening interactions at long range form the basis for this general theory.

Counterion condensation refers to a specific mode of binding of counterions to a polyelectrolyte in which a constant relationship exists between the axial charge density of the polyelectrolyte and the valence of counterions which is valid over a broad concentration range of the counterion species. The concept of counterion condensation is markedly different from association reactions between ion pairs occurring in dilute small electrolyte solutions, in which the extent of ion binding and the tightness of the complex are inseparable. In polyelectrolyte solutions in an environment of a single counterion species, the extent and tightness of binding are uncorrelated. The extent to which condensed counterions are dehydrated or localized, that is, the tightness of binding, can be expected to vary both with the nature of the charged groups on the polyelectrolyte and the counterion species. Condensed counterions which are fully dehydrated are tightly bound by several neighboring charged groups and are said to be localized. Condensed counterions retaining all their water of hydration corresponding to the hydration state in pure water are said to be delocalized. Condensed counterions with hydration states between the two extremes are said to be loosely bound.

Counterion condensation on a polyion occurs when the axial charge density is greater than a critical value. When this condition is met, condensation continues until a saturation point is reached. At this point, the saturated charge fraction, that

is the ratio of counterions to available charged sites, is less than one and is invariant to further increases in the ion concentration in the bulk electrolyte. To quantify this observation, a dimensionless structural parameter Q is defined as proportional to the charge density,

$$Q = \frac{q^2/\varepsilon b}{kT},$$ (1)

where q is the proton charge, ε is the dielectric constant of the bulk medium, k is Boltzmann's constant, T is the absolute temperature, and b is the average axial charge spacing. The value of the saturated charge fraction (q_{net}/q) depends only on the valence of the counterions and the axial charge density of the polyelectrolyte and is equal to $(NQ)^{-1}$, where N is the valence of the counterion. This relation was obtained by minimization of the total free energy of the system against the parameter Θ_N which represents the number of associated counterions per unit charge.

The free energy of the system has two contributions which vary with Θ_N: g_{el}, given by the total work of charging the polyelectrolyte ionic groups against their mutual electrostatic repulsions, and g_{mix}, given by the mixing of free cations, bound cations, and solvent molecules (assuming the polyion is negatively charged). By itself, g_{el} would lead to complete binding, that is $N\Theta_N = 1$; g_{mix} alone would lead to $\Theta_N = 0$. The equilibrium state is determined from minimization of the sum $g_{el} + g_{mix}$. For polyelectrolytes, however, g_{el} increases without bound as the concentration of simple electrolyte, C_N, in the bulk goes to zero. Minimization of the sum $g_{el} + g_{mix}$ leads to a relation which in the limit of C_N vanishing can only be satisfied by values of Θ_N given by

$$N\Theta_N = 1 - (NQ)^{-1}.$$ (2)

Since the normalized effective charge is defined by,

$$\frac{q_{net}}{q} = 1 - N\Theta_N,$$ (3)

where q_{net} is the effective charge on each charged group, equation (2) implies that the charge fraction goes as $1/NQ$. It can be shown from this result, that for $Q > 1$ the polyion is surrounded by a local concentration which is positive even as the concentration of the counterion species in the bulk tends to zero.

Dielectric models based on counterion distribution hypotheses

Only one author (Oosawa[18,19]) has suggested using Manning's theory to obtain predictions about the dielectric behavior of polyelectrolytes. In his treatment, the low frequency dispersion was explained in terms of the relaxation of the polarization of condensed counterions induced by their diffusion along the polyion. The high frequency relaxation was attributed to polarization perpendicular to the polyion. Oosawa concluded that the dispersion parameters are independent of the length of the polyion but increase with concentration suggesting contributions of loosely bound counterions.

In the model introduced by Van der Touw and Mandel,[20] the polyelectrolyte was represented as a sequence of charged rod-like subunits in an arbitrary but fixed configuration. The mobility of the associated counterions along a subunit was assumed to be different from that of counterions moving between subunits. This model predicts the occurrence of two dispersions. The high frequency dispersion was attributed to induced dipole moments due to the distribution of counterions along the subunits, whereas the low frequency dispersion was attributed to the induced dipole moment of the entire molecule and its associated counterions. Since the high frequency relaxation is determined by the response of ions moving within each subunit, its amplitude is independent of the length of the macromolecule and consequently of its molecular weight. It is interesting to note that in a model in which the polyion was represented by a rigid rod, the high frequency dispersion was absent.

Grosse[21] (as part of the work at CUA described below, and in an attempt to explain data obtain in our laboratories) considered a theoretical model specifically developed for the case of DNA solutions, but also applicable to other polynucleotides. His work concentrated on explaining the nature of the high frequency relaxation. The DNA solutions were represented by suspensions of charged cylindrical rods with associated "condensed" counterions from the bulk electrolyte. The response of the "condensed" counterions to a high frequency field was taken to be equivalent to that of a highly conducting layer surrounding the cylindrical particle. With this model, Grosse calculated the dielectric properties of the equivalent homogeneous particle using the mixture formulas derived by Weiner[22] and Rayleigh[23]. For prolate spheroids, which can approximately represent long cylindrical particles, Fricke's extension of the Maxwell-Wagner model to elliptical particles[24] predicts the occurrence of two relaxations, one at low frequencies and one at high frequencies. Using the general method of Reynolds and Hugh[25] Grosse calculated the parameters of the latter relaxation showing that they are independent of any specific absorption mechanism of the particle,

but depend on the fraction of ions which are condensed on its surface.

Dielectric models based on bound water

Experimental studies extending beyond 100 MHz have pointed to the existence of another relaxation between the β dispersion, and the relaxation of pure water (Schwan,[11] Grant et al.[12-18]). This relaxation, called the δ relaxation, which has been observed in proteins such as hemoglobin and myoglobin and in DNA has been attributed, by Grant and co-workers[15] for instance, to the effect of bound water. For the case of myoglobin, Grant pointed out that the experimental data can be fit to obtain two Cole-Cole dispersions, two Debye type dispersions and one Cole-Cole, or four Debye type dispersions. With additional information from X-ray diffraction regarding the shape and size of the molecule, and using mixture relationships based on the Maxwell-Wagner equations (discussed later) with the appropriate model for the hydrated molecule, he concluded that the correct representation was the one yielding four Debye type dispersions. The first two dispersions correspond in this model to the α and β relaxations, the last dispersion was forced to fit that of pure water, and the remaining dispersion which occurs in the low GHz range was attributed to bound water. Grant also pointed out that the bound water model can indeed account for most if not all of the observed relaxations.

The Maxwell-Wagner model for heterogeneous mixtures of spherical particles

If a polyelectrolyte solution is viewed as a heterogeneous mixture, the β dispersion can be attributed to interfacial polarization also referred to as the Maxwell-Wagner effect·[26,27] It is well known that heterogeneous systems of spherical particles dispersed in a continuous phase have relaxations due to interfacial polarization occurring at the boundaries between the components of the mixture. The Maxwell-Wagner derivation considers a system containing spheres of radius a, permittivity ε_p and conductivity σ_p sparsely distributed in a medium of permittivity ε_m and conductivity σ_m. The system is acted upon by an electric field $E = E_o \exp(i\omega t)$. The derivation is carried out in two steps; first Laplace's equation is solved to determine the potential outside an individual particle and the results are extended to solve for the potential surrounding a sphere of radius R>>a which is assumed to contain all the particles, and is surrounded by the continuous phase. Secondly, the same problem is solved for a sphere of radius R, with the properties of the heterogeneous system, immersed in a medium with the properties of the continuous phase. The solutions obtained for the potential outside the large sphere are equated to obtain for the specific admittance K of the mixture (Van Beek[28]) the relation

18

$$K = K_m \frac{2K_m + K_p + 2v(K_p - K_m)}{2K_m + K_p - v(K_p - K_m)} \tag{4}$$

where $v = N(a/R)^3$ is the volume fraction of the dispersed component, $K = \sigma + iw\varepsilon_0\varepsilon$ is the specific admittance or generalized complex conductivity, and ε_0 is the permittivity of vacuum. This equation can also be expressed in terms of complex permittivities $\varepsilon_g = \varepsilon + \sigma/iw\varepsilon_0$ as shown by Grosse[29] as well as in terms of other physical parameters.

The frequency dependence of the permittivity ε and the conductivity σ as obtained from equation (4) shows a single relaxation behavior. Represented in a Cole-Cole plot in terms of real and imaginary parts, ε'' vs. ε' and σ'' vs. σ' appear as semicircles. Using a single relaxation Debye model with ε' and ε'' are given by

$$\varepsilon' = \varepsilon_\infty + \frac{\varepsilon_s - \varepsilon_\infty}{1 + w^2\tau^2}, \tag{5}$$

and

$$\varepsilon'' = \frac{(\varepsilon_s - \varepsilon_\infty)w\tau}{1 + w^2\tau^2} \tag{6}$$

with limiting static (ε_s) and infinite frequency (ε_∞) permittivities,

$$\varepsilon_s = \varepsilon_m \frac{2\sigma_m + \sigma_p + 2v(\sigma_p - \sigma_m)}{2\sigma_m + \sigma_p - v(\sigma_p - \sigma_m)} + 3v\sigma_m \frac{(2\sigma_m + \sigma_p)(\varepsilon_p - \varepsilon_m) - (2\varepsilon_m + \varepsilon_p)(\sigma_p - \sigma_m)}{[2\sigma_m + \sigma_p - v(\sigma_p - \sigma_m)]^2}; \tag{7}$$

and

$$\varepsilon_\infty = \varepsilon_p \frac{2\varepsilon_m + \varepsilon_p + 2v(\varepsilon_p - \varepsilon_m)}{2\varepsilon_m + \varepsilon_p - v(\varepsilon_p - \varepsilon_m)}. \tag{8}$$

The relaxation time τ is given by

$$\tau = \varepsilon_0 \frac{2\varepsilon_m + \varepsilon_p + v(\varepsilon_m - \varepsilon_p)}{2\sigma_m + \sigma_p + v(\sigma_m - \sigma_p)}. \tag{9}$$

In this case, the dielectric parameters are independent of particle size. It must be noted that the limiting values of the permittivities are applicable only with respect to the Maxwell-

19

Wagner effect. When other dispersions are present these values represent intermediate constants between relaxations.

Dintzis et al.[4] postulated that for solutions of polyelectrolytes $\varepsilon_p = \varepsilon_m$ and $\sigma_p \gg \sigma_m$ and indicated that the dielectric increment $(\varepsilon' - \varepsilon_\infty)$ was enhanced as the difference between σ_p and σ_m increased.

Linear polyions can be approximated as prolate ellipsoids of revolution with large values of the axial ratio. O'Konski[30] considered a model for such ellipsoids surrounded by an electrical double layer characterized by a surface conductivity assumed to be large along the particle surface and small along other directions. He derived expressions for the dielectric increment and the relaxation time in terms of components of the depolarization factor A_J and the conductivity, including the contribution of the surface conductivity, along the three principal axes of the ellipsoid:

$$\varepsilon = \frac{1}{3} \, v \, \varepsilon_m \, \sum_j \, \frac{\varepsilon_J/\varepsilon_m - 1 + (\sigma_J/\sigma m - 1) \, A_J}{[1 + (\sigma_J/\sigma_m - 1) \, A_J]^2} \qquad (10)$$

$$\tau = \varepsilon_0 \, \frac{\varepsilon_J + \varepsilon_m (A_J^{-1} - 1)}{\sigma_J + \sigma_m (A_J^{-1} - 1)} \qquad (11)$$

In this case, the dielectric properties are still independent of the size of the particle, but depend on the axial ratio.

O'Konski's model was not adequate to explain the behavior of systems displaying very high permittivities at low frequencies. To describe these cases, Schwarz[31] introduced a frequency dependent surface dielectric constant with a relaxation determined by the diffusion of counterions in the double layer. Takashima[32] extended this model to the case of ellipsoids. In both cases, the Maxwell-Wagner equations still hold with appropriate modifications. Other studies have followed in this area; however, since they concentrate on the origin of the low frequency dispersion they will not be considered here.

(1) Experimental Research

(a) Methodolcgy

Various types of instrumentation have been used to measure dielectric properties of solutions. At frequencies below 100 MHz admittance bridges are commonly used which in principle allow for measurements down to dc. In this case, however, there are practical limitations particularly with conducting solutions, due to electrode polarization effects, which generally occur at low frequencies. With this technique, complex permittivities can be

measured by placing the sample between two plates forming a capacitor. For lossy solutions the system can be represented by a parallel capacitance C_p and resistance R_p. The complex admittance of the circuit is given by $Y^* = 1/R_p + iwC_p$. The complex permittivity of the sample ε^*, is given by

$$\varepsilon^* = \varepsilon' - i (\varepsilon'' + \sigma/w\varepsilon_0) \qquad\qquad (12)$$

where ε' and ε'' are respectively the real and the imaginary parts of the permittivity, σ is the static conductivity, and ε_0 is the permittivity of vacuum. The complex admittance of the capacitor is related to these parameters by (Grant[14])

$$Y^* = iwF [\varepsilon' - i(\varepsilon'' + \sigma/w\varepsilon_0)], \qquad\qquad (13)$$

where F is a geometrical factor for the capacitor. The parameters of interest ε', and ε'' can be calculated from $C_p = F\varepsilon'$ and $1/R_p = F(w\varepsilon'' + \sigma/\varepsilon_0)$. As can be seen ε'' can not be directly obtained except for cases where the static conductivity is zero. For other situations, the static conductivity must be independently measured for instance with a conductivity meter.

A major problem for measurements at lower frequencies is electrode polarization. This effect can sometimes be a problem even in the low MHz range. For situations where electrode polarization is a concern, movable electrodes can be used as suggested by Fricke and Curtis[33] and Schwan and Maczuck[34].
In our research measurements are made using a Hewlett Packard 4194A Impedance/Gain-Phase Analyzer for the frequency range between 100 Hz and 40 MHz. A Hewlett Packard 16451A dielectric cell with movable electrodes is used in this range to alleviate the electrode polarization problem. Other cell configurations are occasionally employed when necessary.

Beyond a few hundred MHz dielectric measurements can no longer be made with the impedance bridge technique. Our approach is to use coaxial lines which can generally be utilized between 50 MHz and 18 GHz. This technique makes use of the reflected signal from a sample located at a defined reference plane along the coaxial line. A wide range of sample configurations are possible. In all cases the sample is placed at the end of a coaxial line having an inner diameter a, an outer diameter b, and a characteristic impedance Z_0. The sample may constitute part of the coaxial line or be placed at the end of the line. Two configurations are used in the measurements: a modified GR-900 connector (Stuchly[35]) and an open ended coaxial line. The GR-900 cell is employed up to 2 GHz, while the open ended coaxial line is employed between 2 and 18 GHz. A Hewlett Packard 8510 Network Analyzer is employed to determine the reflection coefficient in terms of the scattering parameters.

(b) Areas of Study

The argument regarding the interpretation of the experimental results, particularly the origin of the high frequency dispersion still goes on today. One objective of this research is to use the fundamental concepts of the theory of polyelectrolytes proposed by Manning[16-17] to investigate the origin of the high frequency dispersion of specific systems of synthetic and biological polyelectrolytes.

Although one author (Oosawa[19]) previously suggested using Manning's theory to describe dielectric behavior, no systematic investigation has been carried out based on this theory. The parametric nature of the counterion condensation model offers many possibilities to design such a study to test this model. The fundamental notion is that the localized concentration of ions in the vicinity of the polyion chain is much greater than the concentration of ions in the bulk electrolyte, even as the latter goes to zero. Thus, the polyion can be viewed as having two types of counterions, a "condensed" counterion layer whose concentration is (approximately) invariant with the concentration of the bulk electrolyte, and a diffuse counterion layer. The characteristics of these regions will dictate the dielectric behavior of the system. There are several parameters which may be expected to influence dielectric behavior as predicted by this theory, these are: the bulk electrolyte species and therefore its valence, the axial charge density of the polyelectrolyte, the nature of the charged groups on the polyion, and consequently, the level of hydration of the counterions and the tightness of binding, and the concentrations of polyelectrolyte and bulk electrolyte.

Several experimental conditions have been considered. The effect of changes in the level of hydration of condensed counterions are investigated by testing different polyelectrolyte solutions which, while having the same concentration of condensed counterions, exhibit different hydration characteristics. This study (now under way) will yield an understanding of the effect on the dielectric behavior of the tightness of binding of counterions. The results will also be analyzed in terms of the bound water model which attributes the existence of the δ dispersion to hydration layers around the entire macromolecule.

Changes in the permittivity of the solvent or the temperature affect the axial charge density and the mobility of counterions. The effect of the condensed counterion layer on the dielectric behavior is under investigation by increasing the dielectric constant of the solvent or the temperature to the point where no counterion condensation occurs. This condition exists when the thermal energy is greater than the electrostatic energy of interaction between charged groups on the polyion, that is, when $Q \leq 1$.

The effect on the nature of the condensed counterion layer, and consequently the dielectric behavior, of deviations from the linear conformation of the polyion is being studied by considering polymers which can take on various conformations from linear to supercoiled. For the latter case, the Maxwell-Wagner model for spheres is expected to hold.

It has been suggested by Oosawa[19] that the high frequency dispersion is due to polarization in the direction perpendicular to the axis of the polymer. If this is the case, the dielectric increment in this range will vary with the diameter of the condensed counterion layer. Experiments to test this hypothesis are being performed by varying the parameter Q which specifies the volume occupied by the condensed counterion layer, and thus the effective diameter of the polymer.

The experimental effort is concentrated on DNA and a few other representative polymers including various polynucleotides as well as some non-biological polymers such as polyvinyl sulfonate, polyvinyl sulfate, and polyphosphate.

References

1. Jungner, I., Acta Physiol. Scand., 10, Suppl. 32, 1945.
2. Jungner, I., Allgen, L. G., Nature, 163, 849, 1949.
3. Allgen, L. G., Acta Physiol. Scand., 22, Suppl. 76, 1950.
4. Dintzis, H. M., Oncley, J. C., Fuoss, R. M., Proc. NAt. Acad. Sci., 40, 62, 1954.
5. Mandel, M., Jenard, A., Trans. Faraday Soc., 59, 2158, 1963.
6. Sachs, S. B., Raziel, A, Eisenberg, H., Katchalsky, A., Trans. Faraday Soc., 65, 77, 1969.
7. Minakata, A., Imai, N., Biopolymers, 11, 329, 1972.
8. Van der Touw, F., Mandel, M., Biophys. Chem., 2, 231, 1974.
9. Takashima, S., Minakata, A., Digest of Diel. Lit., 37, 602, 1975.
10. Mandel, M., Odijk, T., Ann. Rev. Phys. Chem., 35, 75, 1984.
11. Schwan, H. P., Ann. N. Y. Acad. Sci., 125, 344, 1965.
12. Grant, E. H., Ann N. Y. Acad. Sci., 125, 418, 1965.
13. Grant, E. H., Bioelectromagnetics, 3, 17, 1982.
14. Grant, E. H., Sheppard, R. J., South, G. P., "Dielectric Behavior of Biological Molecules in Solution", Oxford University Press, 1978.
15. Grant, E. H., McLean, V. E. R., Nightingale, N. R. V., Gabriel, C., "Interactions Between Electromagnetic Fields and Cells", Ed. Chiabrera, A., Nicoli, C., Schwan, H. P., Plenum Press, N. Y., 65, 1985.
16. Manning, G. S., J. Chem. Phys., 51, 924, 1969.
17. Manning, G. S., Quart. Rev. Biophys. II, 2, 179, 1978.
18. Oosawa, F., "Polyelectrolytes", Ed. Marcel Dekker, N. Y., 1971.

19. Oosawa, F.,"Interactions Between Electromagnetic Fields and Cells", Ed. Chiabrera, A., Nicoli, C., Schwan, H. P., Plenum Press, N. Y., 297, 1985.
20. Van der Touw, F., Mandel, M.., Biophys. Chem., 2, 218, 1974.
21. Grosse, C., Unpublished work at VSL/CUA, 1988.
22. Wiener, O., Abh. Math. Phys. sachs. Wiess., 32, 509, 1912.
23. Rayleigh, J. W., Phil. Mag., 34, 481, 1892.
24. Fricke, H., Appl. Phys., 24, 644, 1953.
25. Reynolds, J. A., Hugh, J. M., Proc. Phys. Soc. B, 70, 769, 1957.
26. Maxwell, J. C., "Electricity and Magnetism", Vol I, 452, Clarendon, Oxford, 1892.
27. Wagner, K. W., Arch. Electroteck., 2, 377, 1914.
28. Van Beek, L. K. H., Dielectric Behavior of Heterogeneous Systems in "Progress in Dielectrics", Vol 7, London, 69, 1967.
29. Grosse, C., J. Phys. D: Appl. Phys., 18, 1883, 1985.
30. O'Konski, C. T., J. Phys. Chem., 66, 605, 1960.
31. Shwarz, G., J. Phys. Chem., 66, 2636, 1962.
32. Takashima, S., Adv. Chem. Series, 63, 232, 1967.
33. Fricke, H., Curtis, H, J. Phys. Chem., 41, 729, 1937.
34. Schwan, H. P., Maczuck, J., Rev. Scient. Instru., 31, 59, 1960.
35. Stuchly, S. S., Rzepecka, M. A., Iskander, M. F., IEEE Trans. on Inst. and Meas., IM-32, No. 1, 56, 1974.

(2) Experimental Results

This report summarizes the results of the second year of a study of microwave interactions with DNA solutions. The initial interest in this subject was prompted by reports of resonant absorption of microwaves by DNA[1,2]. It was reasoned that relatively small amounts of energy could cause significant damage to the DNA or affect its behavior if the resonances were undamped as indicated by their observation. Recent careful measurements[3,4] including our own[5] have shown that undamped resonances are not present. The microwave absorption by DNA remains of interest, however, because of the fact that the absorption of energy by the DNA and its associated counterions may be proportionately greater than in the surrounding bulk liquid. The relatively high localized absorption may affect the behavior of the DNA and its ability to perform its functions.

To understand the microwave/DNA interaction we have found it essential to characterize thoroughly the chemical composition of our DNA solutions with particular attention to ionic conductors. We have extended the frequency range of our measurements down to the kilohertz range to be able to completely cover the relaxation processes extending into the microwave region. We have completed preliminary measurements of the dielectric behavior of DNA solutions from a few kilohertz to 18 gigahertz. We have concluded that to thoroughly understand the observed behavior it will be necessary to perform a series of measurements in which the ionic species and concentration in the DNA buffer is varied. It is hoped that this will give sufficient information to allow us to choose among available models for explaining the DNA dielectric behavior. This knowledge may in turn lead to suggestions of how electromagnetic energy may affect the biochemical behavior of DNA.

(a) Microwave Absorption in DNA - Measurement Methods

(i) Automatic Network Analyzer with Open Ended Coaxial Probe

The measurement of the dielectric properties of DNA solutions presents several formidable obstacles owing to several properties of DNA which include its relatively low solubility and the difficulties involved in preparing large quantities of purified material. The first of these difficulties requires that the measurement technique be highly sensitive and the second requires that measurements be made in relatively small volumes on the order of a milliliter or less. In part due to these difficulties Edwards et al.[1,2] were led to believe that they had observed resonant absorption in DNA.

To measure the properties of DNA, Edwards et al. used and we have adopted the technique of reflection measurements using an open ended coaxial probe and an automatic network analyzer (ANA).

25

The details of the measurement technique were given in our first annual report[5]. In order to observe any spectra due to DNA in dilute solutions (on the order of 0.1% by weight) it was necessary to subtract a large background due to the buffer solution and observe the difference spectrum which showed a resonance like appearance. In the frequency range where the resonances were observed any geometrical differences between the reference buffer measurement and the sample measurement results in apparent resonances. Such geometrical differences could be a small difference in sample volume or a minor displacement of the measurement probe and sample container. This sensitivity to the geometry of the measurement is an unfortunate consequence of the fact that to extract the signal of interest from the signal detected by the network analyzer substantial corrections to the signal are required. These corrections are required to eliminate effects of signal loss, directivity errors, impedance mismatches and include spurious reflection signals such as from sample containers, connectors etc. If these errors are reproducible then they may be corrected but if they change from sample to sample as would occur if sample volume is changed or if the probe is displaced with respect to the sample container the corrections will be in error and a noisy resonant like appearance will result and be exaggerated in any difference spectrum.

During the first year of this project we were able to duplicate the measurements of Edwards et al.[1,2] but showed that the resonances we observed were simply artifacts which could be manipulated by geometrical means. Although we were unable to find any resonance absorption in DNA we did observe what appeared to be an excess absorption which was largely frequency independent below at least 9 GHz. We began the second year of the project with the intention of examining and explaining this apparent absorption excess. The magnitude of the excess was such that if it were associated with the DNA it meant that a disproportionate fraction of electromagnetic energy falling on the samples would be absorbed by the DNA and its associated counter-ion cloud.

In order to accomplish this task it was necessary to improve on the measurement technique. We had to eliminate the geometrical effects leading to the apparent resonances. We also found that it was necessary to control the temperature of the probe to prevent gradual drifts in the signal during lengthy measurements. Further we found that the ionic content of samples did not agree with the expectations of the suppliers and had to be carefully determined by analysis or controlled by additional sample purification or preparation steps.

To demonstrate that spurious reflections from the sample container could be eliminated we performed calibration and measurement steps in increasingly larger containers until movement of the probe in the sample container between measure-

26

ments no longer produced resonances. We began the tests in our standard 1.5 ml sample tubes and found that to completely eliminate the resonances a 20 liter container was required. This would not be practical for biological samples.

It had been suggested that spurious reflections could be eliminated by using a thin walled sample container surrounded by an absorbing medium[6]. We experimented with a number of containers including finger cots and condoms. The best results were obtained with the thinnest condoms surrounded by a saline solution for absorption. With such an arrangement temperature control and handling of the samples presented difficulties and results were not consistent due in part to the failure of such thin walled containers to maintain any fixed shape. We concluded that this would not be a practical approach.

After further experimentation we found that if great care was taken it was possible to keep the measurement geometry relatively well fixed during the experiments using our original sample arrangement. This consisted of a 1.5 ml polyethylene micro centrifuge tube as the sample container which is placed in a concentric temperature controlled cylindrical jacket. The sample solutions can be placed in the sample container using a syringe fixed with a small plastic tube. The syringe can also be used for removing the sample and rinsing the container without disturbing either the container or the sample probe. Using such a procedure the resonances could be minimized sufficiently to make useful measurements. In Figs. 1 and 2 we show examples of absorption difference spectra made using the old procedures showing resonances and the new procedures showing that the resonances have been largely eliminated.

A second source of error in our early measurements using the ANA were due to temperature drifts and gradients in the coaxial probe. Even after lengthy warmup of the instrument there may be a temperature gradient between the end of the coaxial probe attached to the instrument and the end immersed in the sample. This is particularly true for measurements far from room temperature. We found that this problem could be minimized by thermally insulating the probe from the point of connection to the instrument to within a few inches of the sample end. Near the sample end we added a temperature controlled jacket circulating liquid at the same temperature as the sample and calibration liquids. This produced a stable, reproducible temperature gradient in the probe after equilibrium was reached. Equilibration times on the order of 60 minutes were typical.

(ii) Low Frequency Measurements-Impedance Analyzer

After concluding that resonances were not present we began to concentrate our efforts on the apparent excess conductivity of

27

our DNA samples and on the known but not fully understood relaxation spectra of DNA solutions. Relaxation spectra are generally quite broad, extending over many decades in frequency and thus it was necessary to extend our measurement frequency below the 45 MHz available with the network analyzer. We obtained a Hewlett Packard model 4194A impedance analyzer (an automatic impedance bridge) with a frequency range of 100 Hz to 40 MHz allowing us to cover the dielectric spectrum from 100 Hz to 26.5 GHz with two instruments.

To make conductivity measurements at very low frequencies we purchased a small conductivity probe capable of making measurements with sample volumes on the order of 100 μliter. This allowed us to determine a conductivity very near the DC conductivity of the sample solutions. The probe was carefully calibrated using saline solutions mixed in our laboratories and for which the concentrations were verified by chemical analysis. We found that the nominal cell constant supplied with the probe by the manufacturer was in error by more than 50%. The conductivities of the saline solutions were calculated using an empirical equation due to Stogryn[7].

To make dielectric measurements in the low frequency region we constructed a cell similar in design to one used by Foster[8]. This cell is essentially a parallel plate capacitor with the sample held between the plates. It has platinum black electrodes with a surface area of 0.7 cm^2 and for which the spacing can be varied from 0 to 2.0 cm. The capability of variable electrode spacing allows one to make various measurement corrections for errors such as those due to electrode polarization. Further, one can within limits, by changing the plate separation, adjust the capacitance and resistance of the cell to give values for which the impedance analyzer has good sensitivity. The cell can be temperature controlled by circulating temperature controlled liquid through the body of the cell.

(b)   **Measurements on DNA**

(i)   Dielectric relaxation

For samples of purified plasmid prepared at the NIH as well as commercially purified calf thymus DNA we made measurements of complex dielectric properties from a few kilohertz to 18.5 GHz. DNA concentrations ranged from 0.05% to 0.172% by weight. The measurements above 45 MHz performed with the ANA reproduced those made and reported previously in last years annual report with the exception that the formerly observed resonances were removed using our improved measurement techniques. After the effects of temperature drifts were eliminated and with the addition of our low frequency bridge measurements we were able to verify the

28

presence of a relaxation between 1 MHz and 1 GHz which had been observed by Takashima et al.[9]

The evidence for this relaxation can be seen in the Fuoss-Kirkwood[10] plot in Fig. 3. $\varepsilon_m"$ is taken to be the value of the dielectric loss for water at its relaxation frequency and $\varepsilon"$ is the dielectric loss for the DNA solution. In this plot the approximately linear behavior at high frequencies is due to the relaxation due to water near 17 GHz. The change in slope at the low frequency end of the plot is an indication of a second small relaxation which is attributed to the DNA. To understand the nature of this relaxation we believe it will be necessary to perform a series of measurements on samples as a function of temperature, DNA concentration, ionic species and ionic concentration. These measurements have not been made as yet and we can only say that our observations are consistent with those published by Takashima.

The importance of studying the effect of the ionic content of the solutions is that we believe that the dielectric behavior of the DNA is intimately affected by the ion cloud surrounding the DNA. By changing the ionic concentration and valence of these ions we hope to obtain sufficient data to be able to explain the combined effects of DNA, its surrounding ions and any electromagnetic radiation.

(ii) Conductivity excess

Our early measurements of microwave absorption in our DNA samples indicated an excess absorption due to a conductivity excess which was independent of frequency below at least 9 GHz. The magnitude of the excess varied from sample to sample but was sufficiently large that it was thought that its presence could contribute a possible damage mechanism for DNA due to localized absorption. The supplier of the DNA was under the impression that he was always giving us samples in a standard buffer having 5 mM NaCl, 0.1 mM EDTA and 10mM Tris-HCl. Since the ionic content of the samples was all supposed to be the same, we at first suspected that the DNA itself in the solutions was causing the conductivity excess. Grosse proposed a model in which the counterions might see the DNA molecules as a high conductivity surface with the net result being an increased overall solution conductivity. Preliminary calculations based on this model using preliminary experimental parameters were not able to explain the magnitude of the observed conductivity excess.

Before such a model could be completely tested we had to account for all possible sources of normal conductivity. We first attempted to verify the ionic content of the solutions using chemical analysis. The samples were analyzed for Na and K using a DC plasma instrument. We discovered that the ionic content of the solutions was in general several times that

29

specified by the supplier but was still insufficient to explain the observed conductivity.

The supplier suggested that triethylamine-acetate (TEA) which was used in his purification procedures might contribute to the conductivity. TEA is volatile and should have been removed in one of the concentration steps but there was a possibility that a small amount might remain. We measured the conductivity of TEA and determined the concentrations necessary to cause the excess conductivity. Attempts to verify or disprove the presence of TEA in the samples using IR absorption were unsuccessful due to the small signal for TEA and large background due to water at the possible concentrations. The concentrations of TEA required to explain all of the conductivity excess in the samples was, however, greater than used in the processing of the samples so it was concluded that TEA could not be a major source of the excess.

Toward the end of the current year the use of an ICP mass spectrometer became available for chemical analysis. Survey runs on the samples indicated that several additional ions, Cs, Ba, Cu and Mg, in the samples were contributing to the conductivity excess. When the conductivity of the known ion species plus that due to EDTA-tris were added together the conductivity was still only partially explained. Depending on the sample, the remaining conductivity excess ranged from a few percent to more than 50%. Discussions with our chemical analysis group convinced us that it would not be possible to accurately identify all possible conductive species, especially any organic ones. Further, it is clear from examining conductivity models, that with so many possible minor species contributing to conductivity it is not possible to calculate the conductivity with great confidence. We determined that another approach was needed to determine the effect if any of DNA on the conductivity. We decided that the best approach would be to reduce the ionic concentration in the DNA solutions as much as possible by dialysis and then add back known concentrations of NaCl.

We experimented with the effectiveness of dialysis in removing unwanted ions. By dialyzing for periods up to one week against pure water we found that we were able to reduce the conductivity of the samples to less than 0.005 S/m compared to about 0.5 S/m for undialyzed samples. Chemical analysis indicated that Na levels were less than 0.5 ppm (2×10^{-5} molar). Other ions detected and their concentrations were Mg 0.1 ppm, Cs 1 ppm, and Ba .2 ppm. The estimated conductivity from these known ions, assuming Cl as the common anion, was 5×10^{-4} S/m or about 10 % of what was measured. Either the model we are using is grossly inadequate for calculating the conductivity or their are undetected conductive species. We suspect the later but can not prove it. The equivalent NaCl concentration needed to explain the excess conductivity is on the order of 10 ppm. It is

not unreasonable to assume that some undetected organic or inorganic species are present at such low levels.

The normality of the DNA solutions typical of our samples is about 3 mN. Since dialysis was able to reduce the NaCl concentrations in the DNA solutions to about 1% of this we are assured that the DNA has been effectively stripped of NaCl. If we add back NaCl to a DNA solution by dialysis against a saline solution, we expect the Na ions to preferentially become counterions to the DNA for NaCl normalities less than that of the DNA. If DNA somehow increased the effective conductivity of associated counterions then upon adding NaCl to the solution we should see a greater conductivity increase than when adding that concentration of NaCl to pure water.

We performed a set of experiments beginning with a DNA solution that had been dialyzed against distilled water for seven days. As explained above we found a residual conductivity of 0.005 S/m with about 10% being due to known concentrations of remaining salts. We then dialyzed the solution against saline solutions of 0.0015, 0.005 and 0.015 normality respectively.

After each dialysis the conductivities of the DNA and saline solutions were measured. It was found that in each case the conductivity of the DNA solution increased to a value equal to that of the saline solution plus its original unexplained excess. Ignoring that small excess, the conductivities agreed with the value calculated from the empirical formula of Stogryn for NaCl in pure water. This would indicate that DNA does not strongly affect the low frequency conductivity of associated counterions. Since counterions are expected to be in close proximity to the DNA the local salt concentration and thus the localized microwave energy absorption may be relatively large. This could be important in determining the effect of microwaves on the behavior of DNA. To further understand the relationship between DNA and the counterions it is necessary to study the dielectric relaxation of DNA solutions which we are continuing to do.

(c) Conclusions

The results of our dielectric measurements on DNA from 100 Hz to 18.5 GHz do not indicate any unusual behavior for the DNA. There is evidence, however, for dielectric relaxation between 1 MHz and 1 GHz. Further study of this relaxation is desireable in order to understand the process of electromagnetic energy absorption by DNA and its associated counterions. Since the localized energy absorption in the vicinity of the DNA may be significantly larger than in the bulk it is possible that the biochemical behavior of the DNA would be affected in some way.
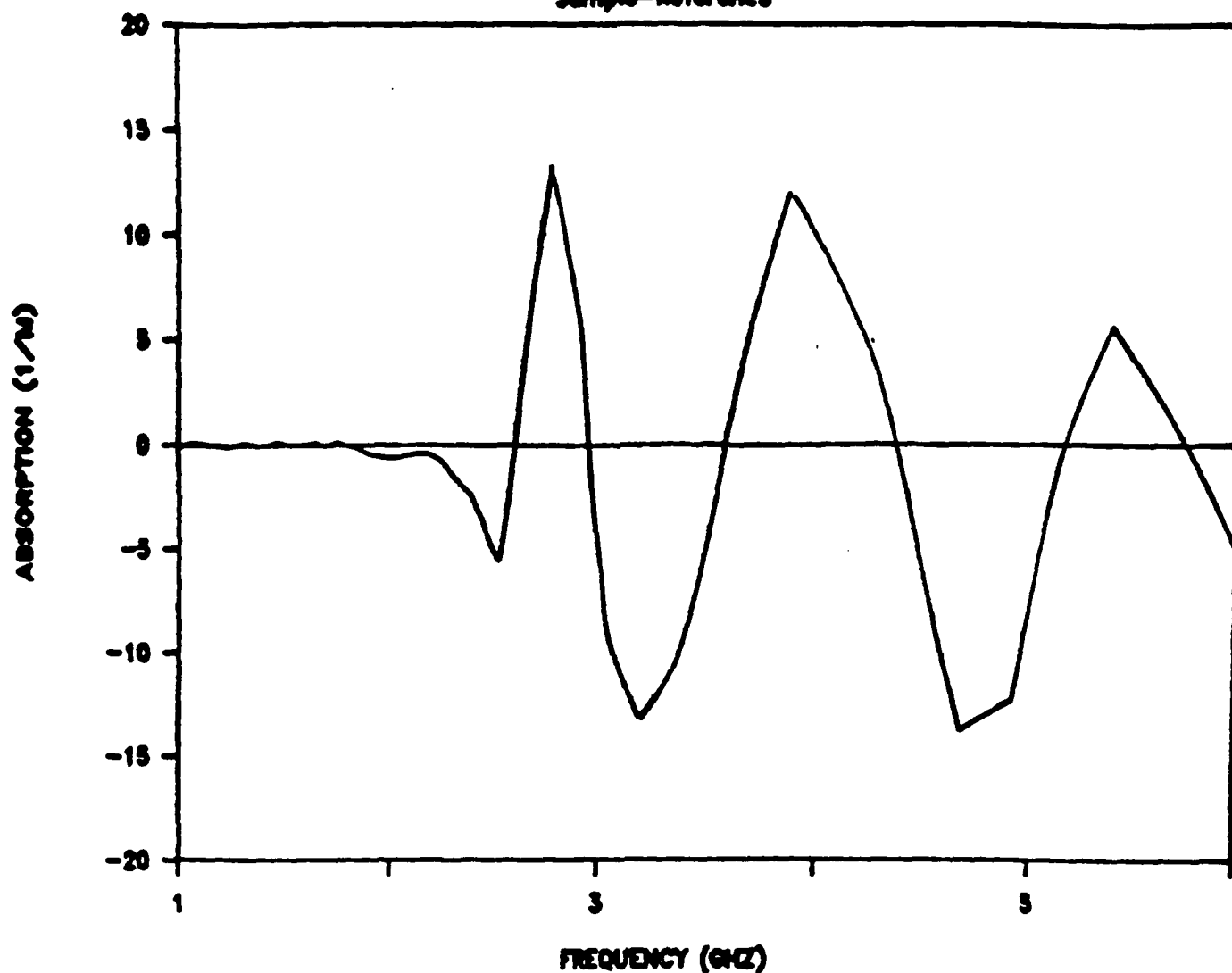
MICROWAVE ABSORPTION

Sample-Reference

Figure 1. The absorption difference spectrum for two water samples. The apparent resonances are due to a volume difference between the two samples.
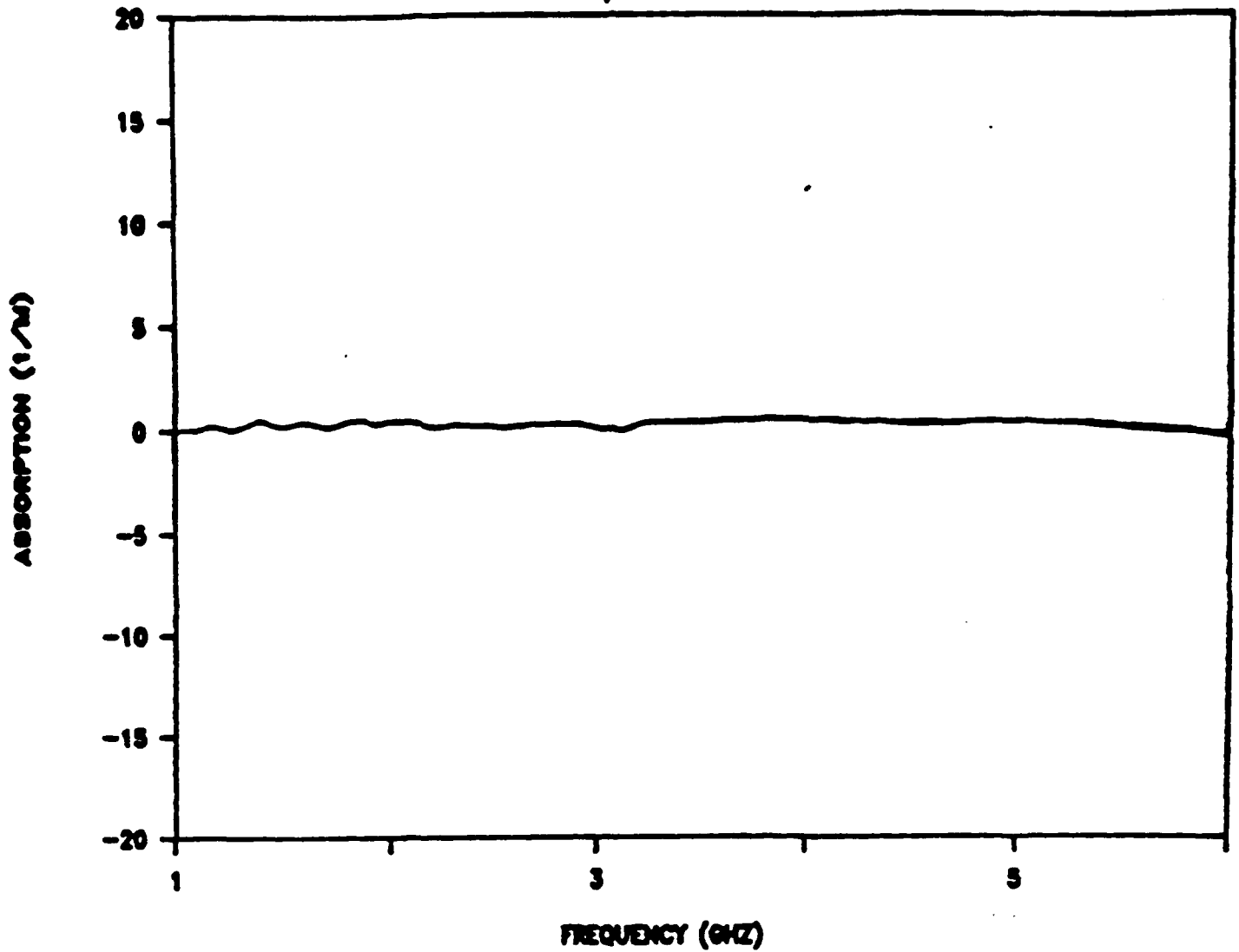
MICROWAVE ABSORPTION

Sample—Reference

Figure 2. The absorption difference spectrum for two water samples for .
which the sample volumes were made as nearly equal as practical. The resonance
are eliminated.

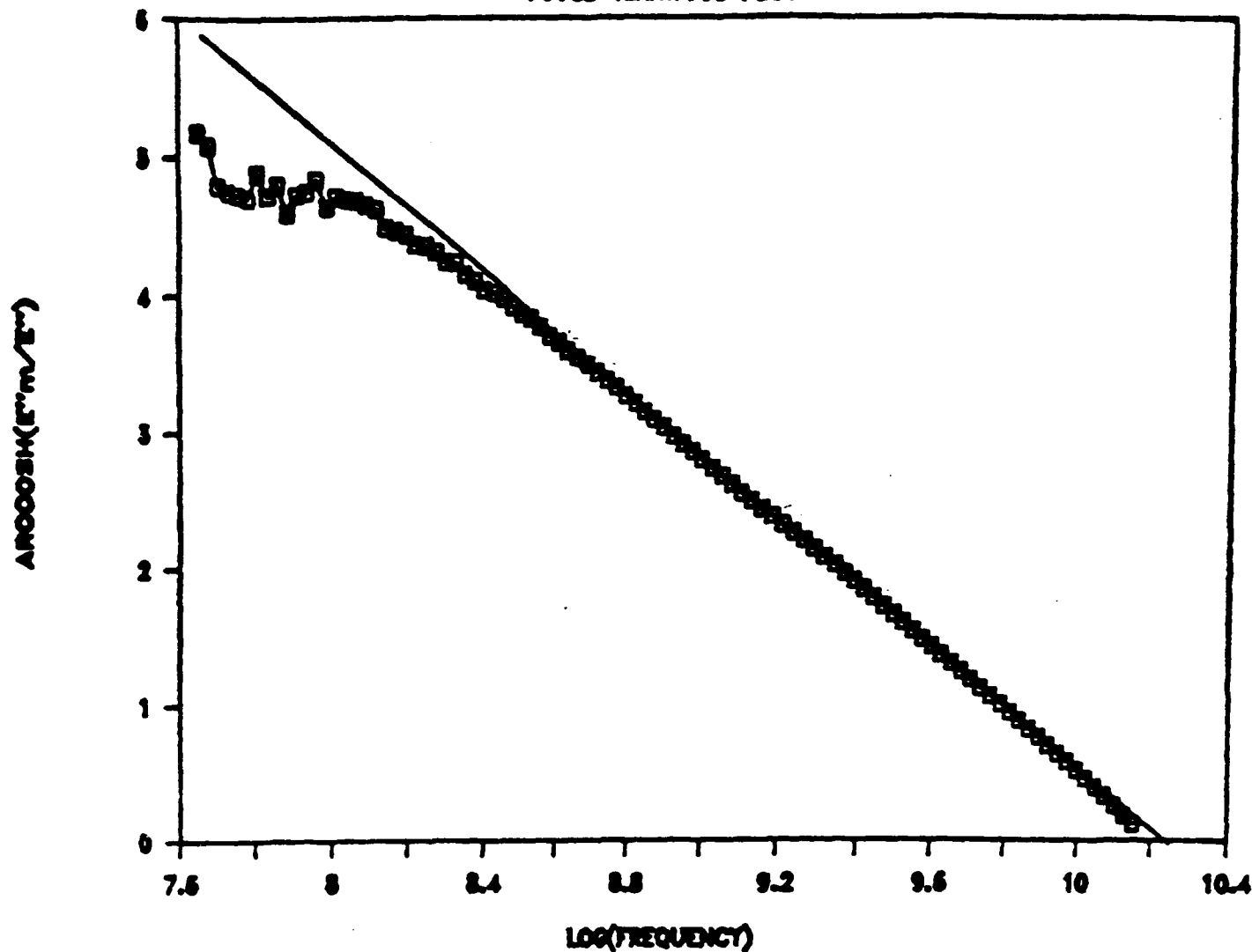# DIALYZED CALF THYMUS DNA

FUOSS-KIRKWOOD PLOT

Figure 3. Fuoss-Kirkwood Plot of a calf thymus DNA sample. The linear portion of the curve indicates the dominant water relaxation near 17 GHz. The change in curvature at low frequencies is attributed to a DNA relaxation.

34

References

1. G. S. Edwards, C. C. Davis, J. D. Saffer, and M. L. Swicord, Phys. Rev. Lett. 53:1284 (1984).

2. G. S. Edwards, C. C. Davis, J. D. Saffer, and M. L. Swicord, Biophys. J. 47:799 (1985).

3. K. R. Foster, B. R. Epstein, and M. A. Gealt, Biophys. J. 52: (1987).

4. C. Gabriel, E. H. Grant, R. Tata, P. R. Brown, B. Gestblom, and E. Noreland, Nature 328:145 (1987).

5. M. Mullins, M. Penafiel, R. Mohr, C. Montrose, T. Litovitz, and C. Grosse, Annual Report Contract DAMD17-86-C-6260 (1988).

6. J. P. Grant, R. N. Clark, G. T. Symm, and N. M. Spyrou, IEE Colloquium Digest #73 London (1986).

7. A. Stogryn, IEEE Trans. Microwave Theory Tech. MTT-19:733 (1971).

8. K. Foster, Univ. of Penn., Philadelphia, Pennsylvania 19104 private communication.

9. S. Takashima, C. Gabriel, R. J. Sheppard, and E. H. Grant, Biophys. J. 46:29 (1984).

10. R. Fuoss and J. Kirkwood, J. Am. Chem. Soc. 63:385 (1941).

(3) Theoretical Efforts

(a) Localized Microwave Heating of DNA Molecules in Solution

The conductivity of a solution of DNA is determined by the free ions in the bulk electrolyte and by the counterions surrounding the charged molecules. The total numbers of these two types of ions can be of the same order of magnitude, so that, when and external field is applied to the system, the generation of heat due to their movements can also be comparable. This raises the question of whether a localized heating of the DNA molecules could occur.

If such an effect did take place, it wold not be the same for all the DNA molecules in the solution because of their different orientation with respect to the applied field. From the biological standpoint, what matters is not the average value of this heating, but rather the maximum temperature increase expected in the most favorable situation. A value of a few degrees would then indicate a possible damage mechanism to biological systems exposed to electromagnetic radiation. Speculation about such localized heating effects have been around for some time.[1]

Calculations of the microwave heating of macroscopic objects immersed in a cooling water bath have also been previously reported.[2] The general conclusion is that a differential temperature rise on the order of 1°C is impossible for molecular size objects. Nevertheless, this conclusion does not exclude, a priori, the possibility of a sizeable heating effect in DNA molecules because of the following considerations:

(a) The above study[2] was analyzed under the assumption that the cooling fluid in contact with the heated object had a constant temperature. The boundary condition is well-suited for experiments in which a circulating fluid is used, but greatly overestimates the heat transfer in the case of a stagnant medium.

(b) For a stagnant bath, the static problem of a heated object can be solved for simple geometries. For a sphere, the temperature increase is proportional to the square of its radius, and it has a negligible value for molecular size objects and any reasonable amount of heat deposition. The situation is totally different for a cylinder: in this case a static solution does not exist--the temperature of the object increases continuously with time. While a DNA molecule cannot be strictly represented by a cylinder of infinite length, so that it must eventually attain a finite temperature, this steady-state temperature difference should be substantially higher than that of a sphere.

36

In order to calculate the temperature increase, two problems must be addressed:

(a)   What is the rate at which energy is deposited in the fluid as a function of the strength and frequency of the incident electromagnetic field? and

(b)   What is the efficiency of thermal transfer to the DNA molecule--and thus the temperature difference--as a function of the rate of heat deposition?

We consider a linear DNA molecule of length L and radius R surrounded by a layer of counterions and immersed in the electrolytic solution. The dielectric properties of the molecule are given by a frequency independent permittivity ε_p. The electric response of the counterions is characterized by a surface conductivity Γ, while the electrolyte is characterized by a permittivity ε_a and a conductivity σ_a.

When an electric field $E_{za\infty} \exp(i\omega t)$ impinges on the system, energy is dissipated by both the ions from the bulk electrolyte and by the counterions. The power deposited on the conductive layer is determined by the surface conductivity and by the _local_ field strength, which strongly depends on the angular frequency ω.

For lower frequencies, the highly conductive region occupied by the counterions tends to expel the field, so that the energy deposition should be low. Maximum deposition is achieved at high frequencies for which the field distribution is solely determined by the permittivities and not the conductivities of the components. Since we are interested in the largest possible effect, we shall confine out attention to this high frequency situation. Two cases are to be considered, those of molecules oriented parallel and perpendicular to the field.

(a)   Molecule Oriented Parallel to the Field

In this case (taking L>>R) the molecule does not perturb the field, so that the field amplitude acting on the counterions is $E_{a\infty}$; therefore the power generated per unit volume of the molecule is

$$P = \frac{2rE_{a\infty}^2}{R} .$$ (1)

(b)   Molecule Oriented Perpendicular to the Field

Here the field inside the molecule is uniform with the value

$$E_p = \frac{2\varepsilon_a}{\varepsilon_p + \varepsilon_a} E_{a\infty} .$$ (2)

Therefore the square of the field acting on the counterions is

$$E_a(r=R)^2 = [\frac{2\epsilon_a}{\epsilon_p + \epsilon_a} E_{a\infty} \sin \theta]^2 + [\frac{2\epsilon_p}{\epsilon_p + \epsilon_a} E_{a\infty} \cos \theta]^2 \qquad (3)$$

where r and θ are cylindrical coordinates. Integrating the power deposition over the surface of the cylinder leads to

$$P = \frac{4rE_{a\infty}^2}{R} \frac{\epsilon_a^2 + \epsilon_p^2}{(\epsilon_p + \epsilon_a)^2} . \qquad (4)$$

Since typically $\epsilon_a \gg \epsilon_p$, the power deposition on molecules oriented perpendicular to the field is about twice that on molecules aligned with the field.

The maximum expected value for the power per unit volume that can be generated on a molecule oriented perpendicular to the field can be estimated as follows. The amplitude of the electric field applied to a system is limited in practice by the electric breakdown strength of air (roughly 10^6 V/m). The field inside the biological system is generally reduced by nearly two orders of magnitude due to the high permittivity of water. This reduction could be partly compensated by the "resonance effect", which occurs when the specimen size is comparable to the wave-length.[3] Thus the maximum field inside the sample should not exceed

$$E_{m-}(max) \approx 10^5 \text{ V/m}. \qquad (5)$$

The surface conductivity Γ can be estimated from the number of elementary charges per unit length along a DNA molecule[4] (0.59 $\cdot 10^{10}$ charges/m) and the value $R \approx 10^{-9}$ m. This gives a surface charge density of about one elementary charge per 100 Å^2, which is about the maximum value attained by surface charge densities in solution. Using a diffusion coefficient $D \approx 2 \cdot 10_{-9}$ m^2/s then leads to

$$\Gamma \approx 5 \cdot 10^{-8} \text{ S}. \qquad (6)$$

The heat generated per unit volume in a DNA molecule could therefore attain a maximum value of

$$P \approx 2 \cdot 10^{12} \text{ W/m}^3 . \qquad (7)$$

The calculation of the temperature of a uniformly heated object in a stagnant cooling bath can only be carried out analytically for a few simple geometries. For a sphere the temperature rises monotonically with time and tends to an asymptotic limit which coincides with the solution of the static

problem. The result for the temperature difference between the surface of the object and the initial temperature of the entire system is[5]

$$\Delta T = PR^2/3\kappa \qquad (8)$$

where κ is the thermal conductivity of the cooling bath ($\kappa = 0.6$ W/m-deg for water). This result shows that for spheres with radii less than one 1μm, a temperature rise of 1°C <u>cannot</u> be attained.

For a spheroid, the final temperature difference has a simple form only in the case when the object is a perfect conductor so that the temperature inside it is uniform. In that case

$$\Delta T = \frac{PR^2}{6\kappa e} \ln \frac{1+e}{1-e} \qquad (9)$$

where the eccentricity e is

$$e = [1 - 4R^2/L^2]^{\frac{1}{2}}. \qquad (10)$$

This result diverges when e tends toward unity, showing that the final temperature difference <u>can be arbitrarily large</u> for a sufficiently elongated spheroid. However in this case the time that is required to reach the final state also diverges. Consequently it is necessary to examine the time dependence of the temperature change.

The result takes a relatively simple form if was consider an infinitely long perfectly conducting cylinder. The asymptotic form valid for t >> τ is

$$\Delta T(t) = \frac{PR^2}{4\kappa} \ln \frac{t}{\tau K} \qquad (11)$$

where $K = 1.7811... = e^{\gamma}$ ($\gamma = 0.57721 ... =$ Euler's constant) and

$$\tau = \rho C R^2/\kappa, \qquad (12)$$

in which ρ is the density of the external medium and C is its specific heat. For DNA molecules in an aqueous solution $\tau \approx 7 \cdot 10^{-12}$ seconds.

Equation (11) clearly constitutes the upper limit for the temperature increase in a molecule, since, for any object of finite length, the temperature must reach a limiting value. The maximum expected temperature difference for a DNA molecule of

infinite length is plotted in Figure 1 as a function of time. The two horizontal lines correspond to the limiting values for a sphere of the same radius and for an ellipsoid with L/R - 1000. The conclusion is that despite the large amounts of power per unit volume that can be deposited on a DNA molecule in solution, no appreciable temperature difference can ever be achieved because of the rapid transport of energy away from an object of so small a radius.
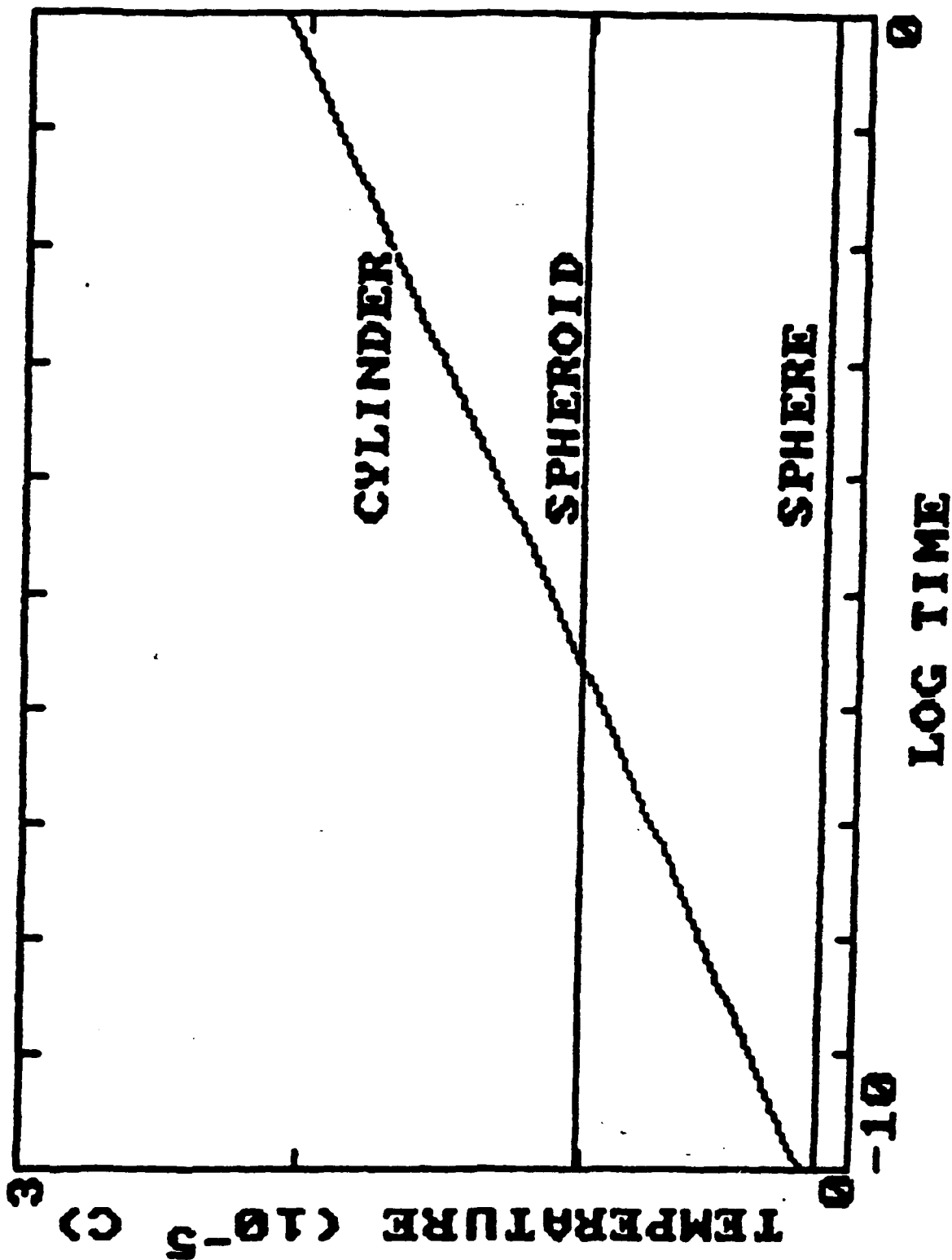
Figure 1. The time variation of the temperature difference for an infinitely long cylinder immersed in an aqueous solution. The horizontal lines show the limiting values for a sphere of the same radius and for an ellipsoid with L/R = 1000.

References

1. R. Kovac, <u>Electrotherapy and Light Therapy</u> (Lea and Febiger, Philadelphia, 1938).

2. K. Foster, P. Ayyaswamy, T. Sundararajan and K Ramakrishna, IEEE Transactions MTT <u>30</u>, 1158 (1982).

3. H. Bassen in "National Safety News" (October, 1980), p. 57.

4. M. Parodi, B. Bianco and A Chiabrera, Cell Biophysics <u>7</u>, 215 (1985).

5. H. Carslaw and J. Jaeger, <u>Conduction of Heat in Solids</u>, 2nd edition (Clarendon Press, Oxford, 1958).

(b)   Microwave Absorption by Suspensions of DNA-type Particles

A theoretical study of microwave absorption by a suspension of charged rod-like particles in an electrolytic solution has shown that due to the concentration of ions around the particles, the absorption of the suspension is frequency dependent, and will always exceed at high frequencies the absorption that would occur if the ions were uniformly distributed.

In addition, it has been found that the dielectric behavior of the simplest possible model of a suspension of charged cylindrical particles is characterized by a relaxation in the microwave region. The parameters of this relaxation are independent of any specific absorption mechanism, but depend on the fraction of the ions which are condensed on the surface of the particles.

This relaxation has its origin in the frequency dependence of the field distribution inside the suspension. At low frequencies the distribution is governed by the relative conductivities of the medium and the particles. The field tends to be excluded from the counterion layer because of its high conductivity, and is concentrated in the bulk electrolyte. This reduces the average current density in the suspension, so that the conductivity falls below the value it would have in a uniform ionic solution.

For frequencies above the relaxation, the current densities are unable to develop appreciable charge densities on the boundaries. The field distribution is then independent of the conductivities, depending rather on the permittivities of the two phases. The field is enhanced inside the particles because of their relatively lower permittivity, and thus the field near the particle's surface (where the condensed ions are located) is also enhanced.

The net effect is that the energy per unit volume deposited near the surface of a DNA molecule can be up to 100 times larger than elsewhere in the ionic medium.

(c)   Dielectric Properties of Particles in Electrolytic Solutions

The three paragraphs below are abstracts of completed theoretical projects which are pertinent to understanding the mechanism(s) of microwave absorption by solutions of DNA or other polyelectrolytes.

i)   Permittivity of a Suspension of Charged Cylindrical Particles in an Electrolytic Solution (by C. Grosse, to be published in the Journal of Physical Chemistry)

43

A simple model recently developed for the low frequency permittivity of suspensions of charged spherical particles in electrolyte solutions [C. Grosse and K. R. Foster, J. Phys. Chem. 91, 3073 (1987)] is extended to the case of cylindrical particles oriented perpendicular to the applied field. Expressions for the conductivity and permittivity as functions of frequency are deduced. The indicate that while the relaxation occurs at essentially the same frequency as in the spherical particle case, the low frequency behavior is totally different. The low frequency conductivity of a suspension of cylindrical particles has the same value as the conductivity of the electrolyte. The low frequency permittivity diverges logarithmically, while its value at any frequency scales with the conductivity of the electrolyte.

ii) On the calculation of the Dielectric Properties of Suspensions (by C. Grosse, to be published in the Journal of Ferroelectrics)

The dielectric properties of suspensions are usually calculated from the quasi-static solution of the Laplace equation for the potential around a single particle in the continuous phase. The results are only straightforward for the static conductivity and for the high frequency permittivity, since these expressions only involve the potentials which are in phase with the applied field. The static permittivity and the high frequency conductivity are much more difficult to evaluate since they depend strongly on the limiting behavior of the out-of-phase terms, which actually vanish in these two limits. Using arguments based on the stored energy and on the dissipated power, it is shown how expressions for these properties can be calculated sing only the in-phase terms of the potential. The results are much easier to derive than those using the classical procedure, and they contribute to a better understanding of the meaning of the relaxation amplitudes. A further advantage of this method is that it permits one to obtain the limiting solutions for the dielectric properties in some systems (e.g., ellipsoidal particles surrounded by a layer of uniform thickness) for which an analytical solution of the Laplace equation does not exist for all frequencies.

iii) On the Extension of Maxwell's Mixture Formula to Ellipsoidal Particles (by C. Grosse, to be published in the Journal of Ferroelectrics)

Fricke's generalization of Maxwell's mixture formula to the case of ellipsoidal particles is reexamined. It is shown that this generalization is based on two approximations which are not justified in the case of randomly oriented particles with high eccentricity. A new expression which avoids this objection is derived. It tends to Fricke's result at low volume fractions, but reduces to the Maxwell formula for very high concentrations.

When particularized to the case of needle-shaped particles, it shows significant deviations from Fricke's formula, which are in qualitative agreement with the extant experimental data.

B. Coupling of Microwave Energy into DNA Molecules

It seems clear from the preceding paragraphs that mechanisms exist and seem to be operative in which the dissolution of a polyion by an ionic solvent leads to enhanced absorption of electromagnetic (microwave) energy by the solution. The question which we now address is whether microwave energy can be directly coupled into the internal degrees of freedom of such polyions, in particular DNA. In the microwave frequency region, i.e., from 1 to about 20 GHz, theoretical considerations lead one to expect the existence of longitudinal vibrational modes of the DNA backbone.[1,2] It has been hypothesized that these modes should couple to and thus produce resonant absorption of irradiating electromagnetic energy.

(1) Resonances: Past Results

In 1984 and 1985 Edwards, Davis, Saffer and Swicord[3,4] (EDSS) reported the observation of relatively sharp peaks in the microwave absorption spectrum of aqueous DNA solutions in the frequency region of roughly 1 to 10 GHz. These observations were surprising and controversial because it had been believed that the strong coupling between the polymer and the viscous solvent would damp any resonant modes.[1,2] Attempts to replicate these results both in our laboratory[5] and elsewhere[6] have led to the conclusion that they are experimental artifacts, unrelated to the normal "organ-pipe" modes of the DNA molecule. It seems apparent that the above mentioned reservations about the damping effect of solvent-DNA coupling on the existence of microwave absorption peaks were well-founded.

(2) Microwave Measurements

The existence of resonant modes in polymers has been observed in crystalline fatty acids and indeed in normal alkanes.[7] We have adopted the Dorfman-Van Zandt hypothesis that the failure to observe these modes in DNA in solution stems from their being quite heavily damped through strong coupling to their viscous surroundings. The important quantity in determining this coupling is the product of the mode frequency with the viscous relaxation time of the solvent. For aqueous solvents, this product is on the order of 0.1, and thus this coupling is rather strong and as a result the vibrational modes are not observed.

The difficulty is, of course that lower viscosity (and thus shorter relaxation time) solvents are simply not available. However it should be possible to reduce the coupling between the DNA modes and the solvent by _increasing_ the viscosity of the latter. In the oversimplified but still representative case of a single viscous relaxation time, the damping of a vibrational mode is proportional to

46

$$\frac{\omega\tau}{1 + (\omega\tau)^2}.$$

Observe that this function is a maximum for $\omega\tau = 1$. Note particularly that for $\omega\tau \gg 1$, this factor falls off as $1/\omega\tau$; thus by increasing the solvent viscosity, η, and consequently the relaxation time τ (since $\eta = G_\infty \tau$), the damping can be decreased. We have initiated a program to investigate the effect of solvents whose relaxation times can be varied by changing the temperature to see if these longitudinal resonances an be detected.

(3) Raman Scattering Studies

The same kind of thinking allows one to recognize that if one increases ω sufficiently, a similar result can be achieved. To accomplish this, we have also initiated a program to study the Raman spectra of shorter polymers of the type studied by Vergoten et al. such as stearic acid. In contrast to their work which was carried out in the pure crystals, our studies would be performed in relatively dilute solutions. The aim of this work is twofold: (1) to establish that the damping of the resonant modes does indeed vary with frequency and relaxation time as suggested above, and (2) to establish the appropriate parameters (e.g., τ) for a range of solvents as a function of such properties as temperature and salt concentration.

References

1. B. H. Dorfman and L. L. Van Zandt, Biopolymers 22, 2639 (1983).

2. L. L. Van Zandt, Phys. Rev. Letters 57, 2085 (1986).

3. G. S. Edwards, C.C. Davis, J. D. Saffer and M. L. Swicord, Phys. Rev. Letters 53, 1284 (1984).

4. G. S. Edwards, C.C. Davis, J. D. Saffer and M. L. Swicord, Biophys J. 47, 799 (1985).

5. M. Mullins et al. "Mechanisms of Microwave Induced Damage in Biologic Materials", Annual Summary Report, WRAIR Contract No. DAMD17-86-C-6260, January, 1988.

6. Kenneth R. Foster, private communication

7. See for example G. Vergoten, G. Fleury and Y. Moschetto, "Low Frequency Vibrations of Molecules with Biological Interest," in Advances in Infrared and Raman Spectroscopy, Volume 4, ed. R. J. H. Clark and R. E. Hester (Heyden and Sons, Ltd., London, 1978) Chapter 5.

3. Design and Evaluation of Microwave Irradiation Systems

A. Microwave irradiation system for exposure of biological cell at 2.45 GHz.

1. System description

The original exposure system described in section 1.2.1 of the first annual report was modified to consist solely of coaxial components except for the applicator. The term 'applicator' refers to the section of waveguide were the sample is loaded for irradiation. A block diagram of the system is shown in Fig. 1. The incident power and the reflected power are measured at the outputs of the first and second 20 dB coaxial couplers respectively. The transmitted power is measured at the output of the applicator. Since the sample represents a mismatch in the line, optimum energy coupling is obtained by adjusting the double stub tuner to minimize the reflected power.
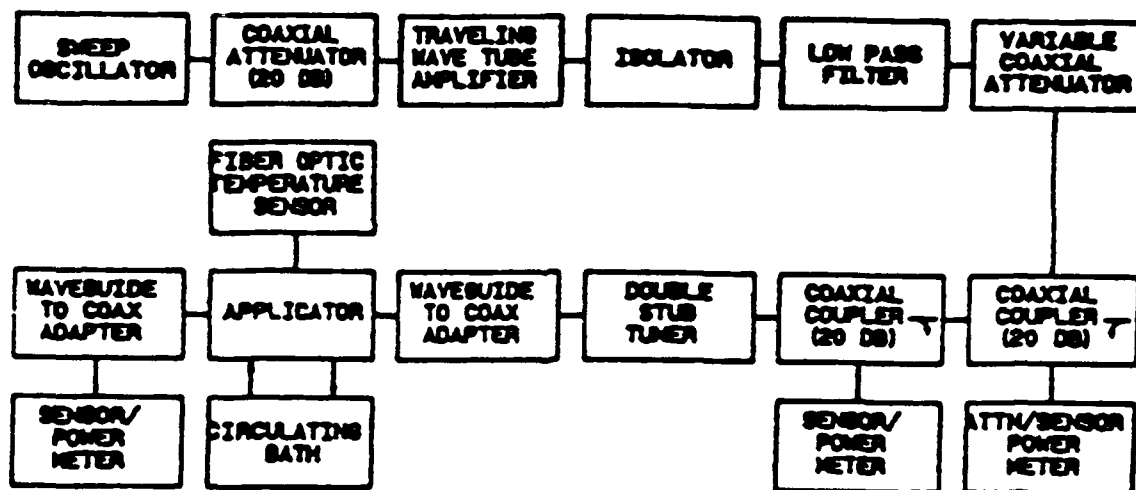

Fig. 1: Block diagram of system for microwave exposure of biological cells at 2.45 GHz.

2. Applicator design

To alleviate some problems with temperature uniformity and settling of the cell suspensions, the original applicator was modified such that the sample tube extends out through both the top and the bottom of the waveguide. This configuration leads to a more uniform electric field distribution within the portion of the sample tube inside the waveguide and allows the use of a magnetic stirring bar which rotates at the bottom of the sample tube to maintain the cells in suspension. The action of the magnetic stirring bar also reduces temperatures gradients within the sample. Temperature measurements along the long axis of the sample tube showed temperature uniformity to within .2°C at a nominal SAR of 400 mW/g. 1 cm O.D., 3.6 ml polyethylene sample tubes with screw cap tops are used as sample containers. Cooling is provided by circulating silicone oil DC200/5 through a sealed bath surrounding the sample tube. This fluid is nontoxic, chemically inert, and essentially lossless. Fig. 2 shows a longitudinal cut along the center of the applicator. The sample temperature is monitored during exposure with a fiber optic Luxtron probe inserted trough the cap of the sample tube.
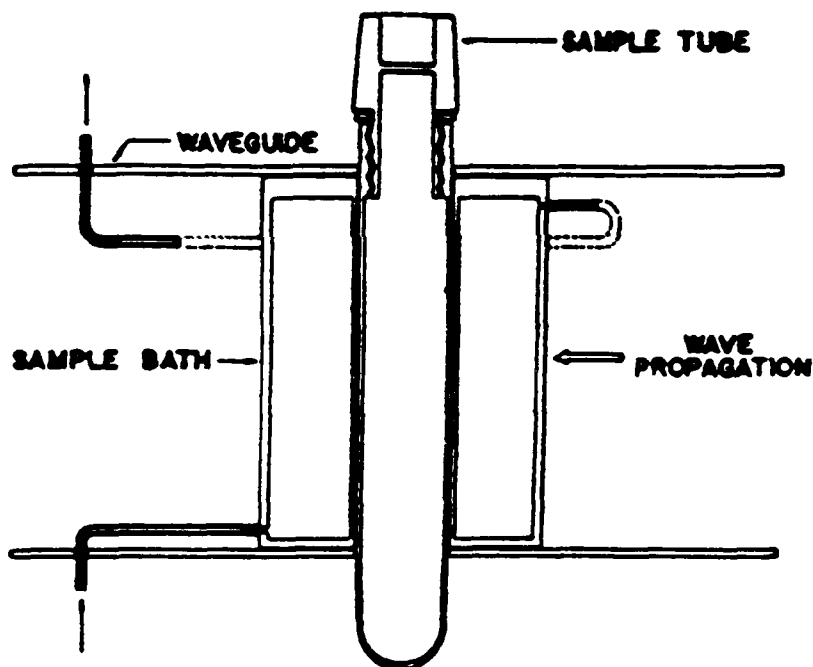

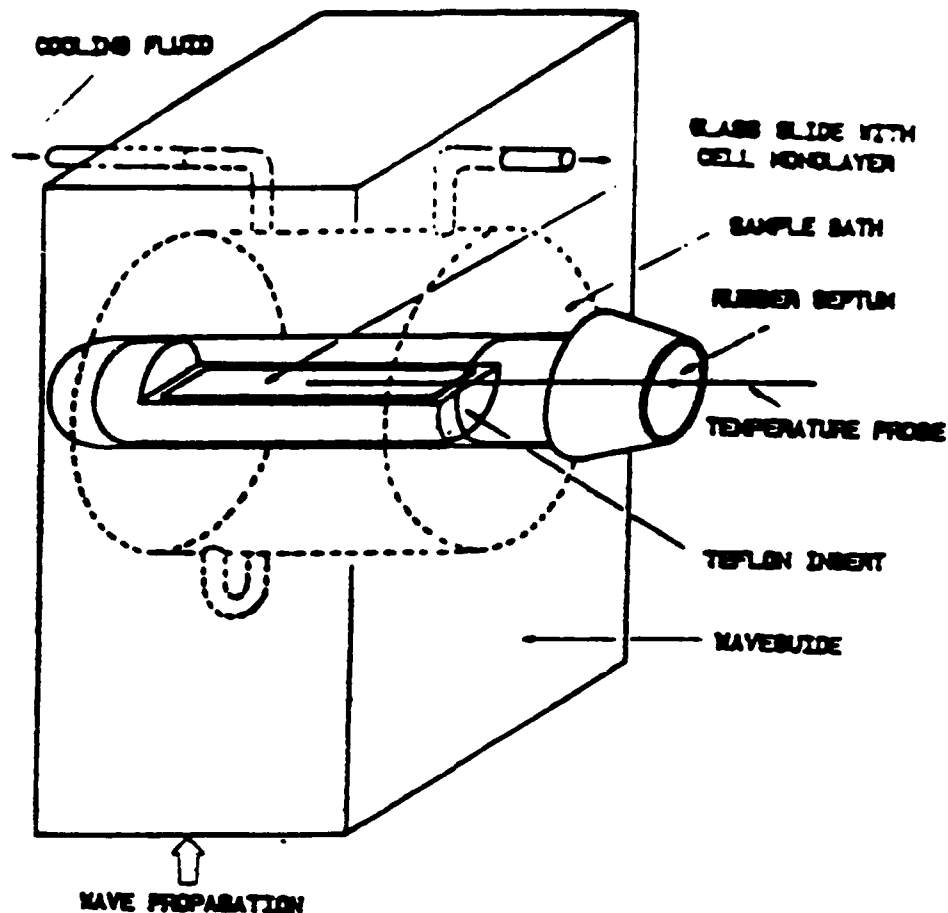Fig. 2: Longitudinal cut along applicator loaded with sample tube.

Fig. 3: Applicator configuration for irradiation of attached cells.

A plexiglass box was built around the applicator to provide some atmospheric isolation and allow flow of a controlled atmosphere of 95% air and 5% CO_2 which was found to be necessary to achieve pH stability during long time runs, e.g. overnight exposures. For greater effectiveness, the air/CO_2 mixture is delivered into a polystyrene vial positioned upside down over the sample tube inserted in the applicator.

The same applicator was used for exposure of cell monolayers attached to a glass substrate. In this case a teflon insert is placed in the sample tube to hold the glass slide containing the sample. The applicator is positioned as shown in Fig. 3. The sample temperature is monitored during exposure with a fiber optic Luxtron probe inserted through a septum in the cap of the sample tube and located directly over the cell monolayer.

Applicators identical to those described above but not connected to a microwave signal were used for sham exposures.

50

3.   SAR measurements

The Specific Absorption Rate (SAR) may be expressed as $SAR = C_p(dT/dt)$ where C_p is the specific heat of the irradiated sample and dT/dt is the rate of increase of temperature per unit time within the irradiated sample. Since temperature is measured as a bulk property, it is clear that the SAR determined using this definition is a measure of energy deposition in the bulk medium and not necessarily in the cells suspended in the medium or the cells bathed by the medium for the case of attached cells. Bearing this in mind, the SAR is not sufficient to specify a given experimental condition without knowledge of the volume of medium exposed. This is particularly true for the case of exposure of monolayers.

SAR measurements for the cell suspension case were carried out by monitoring dT/dt in response to an incident signal of 15 Watts at various positions along the center axis of the sample tube within the waveguide. The SAR measured at points where the sample tube crosses the walls of the waveguide was lower by about 40% than that measured at the center. This is probably due to heat loss since the ends of the sample tube were not insulated during the measurement. If the true value of the SAR is taken to be the value measured close to the center of the sample tube, the SAR for this configuration can be approximately expressed as: SAR = P_{NET}[mW]/[g]. This represents a value of the SAR within the waveguide. The average SAR would be lower since the sample extends outside the waveguide and circulates within it at a rate determined by the rotation of the magnetic stirrer. The average SAR is estimated to be approximately three fourths of the measured SAR since at any given time only three fourths of the sample are inside the waveguide.

Similar measurements were carried out for the cell monolayer case. The sample container was completely filled with nutrient medium making sure no air bubbles were left inside. Again, the SAR measured at points where the sample tube crosses the walls of the waveguide was lower by about 40% than that measured at the center. The SAR for this configuration, taken to be the value measured at the center of the tube, can be approximately expressed as: SAR = $1.2 * P_{NET}$[mW]/[g].

It must be noted that SAR values for experiments with cell suspensions reported in the quarterly reports covered by this reporting period were specified based on SAR measurements performed on the original applicator configuration. With the new applicator energy coupling into the sample is considerably more efficient. According to the new SAR calibration the reported SAR values should be increase by a factor of three. Thus, experiments nominally carried out at 100 mW/g were actually carried out at 300 mW/g. Similarly, the SAR values reported for experiments with attached cells using the new applicator should be increased by a factor of 4.8.

51

B.   Summary of studies carried out using the 2.45 GHz irradiation
      system.

      Various studies were carried out during this reporting period
using the 2.45 GHz irradiation system with both CW and pulsed
microwaves.   These are   summarized below.   Details of each experi-
ment are reported elsewhere in this report.

1.   Effects of 2.45 GHz CW microwaves on two interferon regulated
enzymes, 2'-5' oligoadenylate (2-5A) synthetase and 2-5A dependent
endoribonuclease (RNase L) in murine L929 cells.   Exposures were
conducted for 4 hours at 37°C.

2.   Studies of CW microwave induced changes in cell cycle profiles
between 37°C and 41°C.

3.   Studies of microwave induced dome formation in confluent
monolayer cultures of LLC-PK pig kidney epithelial cells with both
CW and pulsed microwaves.

4.   Effects of CW and pulsed microwaves on cell viability and
ornithin-decarboxylase and RNase L activities in HL-60 human
leukemic lymphocyte cells in suspension. Short term and long term
(24 hr.)
exposures were conducted at 37°C.

C.   Studies of the effects of low level microwave radiation on the
      activity of enolase.

      A series of experiments were carried out at Howard University
in collaboration with Dr. S. K. Dutta to study possible effects of
low level (0.12 mW/g) microwave radiation on the activity of
enolase, an important enzyme of the glycolithic path. This work
involved the use of a Crawford cell with compartments within which
2 small culture flasks (25 cm²) could be placed, one at either side
of the center conductor.   The experiments were carried out with
NG108 clone cells grown attached to one of the large surfaces of
the flasks and used when a confluent culture was obtained.   The
cells bathed in 5 ml of nutrient medium were irradiated in the
Crawford cell such that the microwave signal passed first through
the cell layer and then through the medium. All experiments were
performed at 915 MHz with 16 Hz (80%) modulation for a 30 minute
exposure at 37°C. Two exposed and two control samples were used.

      After irradiation the enolase assay was conducted on sham and
exposed samples by spinning down the cells in a table centrifuge,
homogenizing, removing the cell debris by centrifugation and using
the remaining cell extract to react with 2-phospo-glyceric acid in
a reaction buffer to form phosphoenolpyruvate, a compound with an
absorption peak in the UV.   The kinetics of the reaction were

observed for 3 to 6 minutes by monitoring with a spectrophotometer the increase in the absorption peak of phosphoenolpyruvate at 240 nm. To obtain the specific enolase activity in (µM product/min)/(µg protein) the absorption at 280 nm corresponding to the protein concentration was also measured.

Our observations indicated that several corrections and improvements to the original experimental method were needed in order to validate the results. A main point of contention was the validity of the cellular protein determination. Since the cells were maintained in a medium containing approximately 10% protein, we advised that a rinsing step was desirable prior to homogenization to remove the extracellular proteins. Rinsing with polyphosphate buffer saline by mixing with a vortex was found to be undesirable due to possible rupturing of the cells by the vortexing action. Although several methods were tried, it was not possible to devise an acceptable technique in the time available to effectively carry out this step. The protein assay method which consisted of measuring the absorption at 280 nm, also came under question due to interferences from absorptions present in that region of the spectrum due to other entities present in the cell extract, such as nucleotides. It was suggested that the Bradford method for protein determination be used. This method which utilizes a reaction with proteins yielding a product with an absorption at 595 nm is generally considered to be more accurate.

Thirteen experiments were carried out five of them without the additional rinsing step. For the latter case the results show a consistent increase in the enolase specific activity of the exposed samples compared to the controls (Table I). This evidence has led us to conclude that, in spite of experimental inconsistencies, the observed effect appears to be real. However, it should be pointed out that there is a need for better controlled experiments in this area.

TABLE I. Ratio of the specific activity of enolase in the exposed over the control samples.

Exp ID	E/C[1]	E/C[2]
1	2.245 ± 0.735	---
2	1.233 ± 0.180	---
3	1.440 ± 0.114	---
4	1.448 ± 0.335	1.304 ± 0.305
5	1.122 ± 0.064	1.102 ± 0.102

1. Protein determined by absorption @ 280 nm.
2. Protein determined by Bradford method.

D.   Microwave irradiation system for exposure of cell monolayers using a Crawford cell.

The system described in section 1.2 for exposure of cell monolayers can be used to irradiate cell cultures of up to 2.5 cm². Bioassay techniques used to investigate the effects of the radiation at specific end points often require a larger number of cells than that which can be found in a 2.5 cm² monolayer. To overcome this difficulty, a new microwave irradiation facility was set up to allow exposure of cell monolayers of up to 100 cm². This system makes use of a Crawford cell for the exposure chamber. The system block diagram is shown in Fig. 4. With the components presently in use the system can operate between 800 and 1000 MHz with a maximum incident power of 10 Watts limited by the use of a 10-Watt TWTA unit. The signal generator (HP 612A) can be operated in CW mode, with internal modulation of 400 Hz or 1000 Hz, and with external modulation including pulsed signals.

The Crawford cell, model IFI CC110, was fitted with shelves positioned parallel to the electric field at either side of the center conductor. Two doors for sample insertion were placed on either side of the Crawford cell perpendicular to the center conductor, and on opposite sides of it. The Crawford cell mounted vertically on a rotating stand was placed in an incubator. Rotary coaxial joints were connected at both input and output ports of the Crawford cell to allow free rotation of the cell permitting access to the sample insertion doors from the front of the incubator. During exposure, sample containers are placed symmetrically at either side of the center conductor to maintain symmetry of the electric field within the Crawford cell.
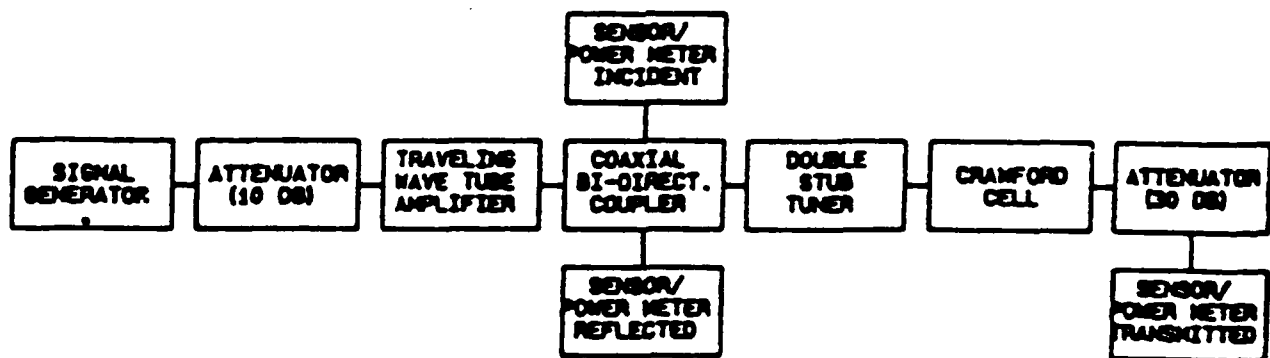

Fig. 4:   Block diagram of system for microwave exposure of cell monolayers using a Crawford Cell.

54

SAR measurements were carried out using 25 cm² tissue culture flasks. Four flasks were used placing two at either side of the center conductor of the Crawford cell. The effective SAR at various power levels was calculated by making measurements of the incident, reflected, and transmitted power to compute the net power loss under two conditions: a) Crawford cell loaded with four empty tissue culture flasks, and b) Crawford cell loaded with four tissue culture flasks filled with 5 ml of nutrient medium. The SAR in the medium was determined from the ratio of the difference of the net power loss under conditions a) and b) to the total volume of the sample (20 ml). A linear regression was performed on the measured data to obtain the following functional relationship between SAR (mW/g) and incident power (mW): $SAR = 3.74 * 10^{-3} * P_{INC}$. Results are shown in Fig. 5. It must be noted that these SAR measurements are valid only for the condition described above and are representative of power deposition within the bulk nutrient medium and not necessarily within the cell monolayer.

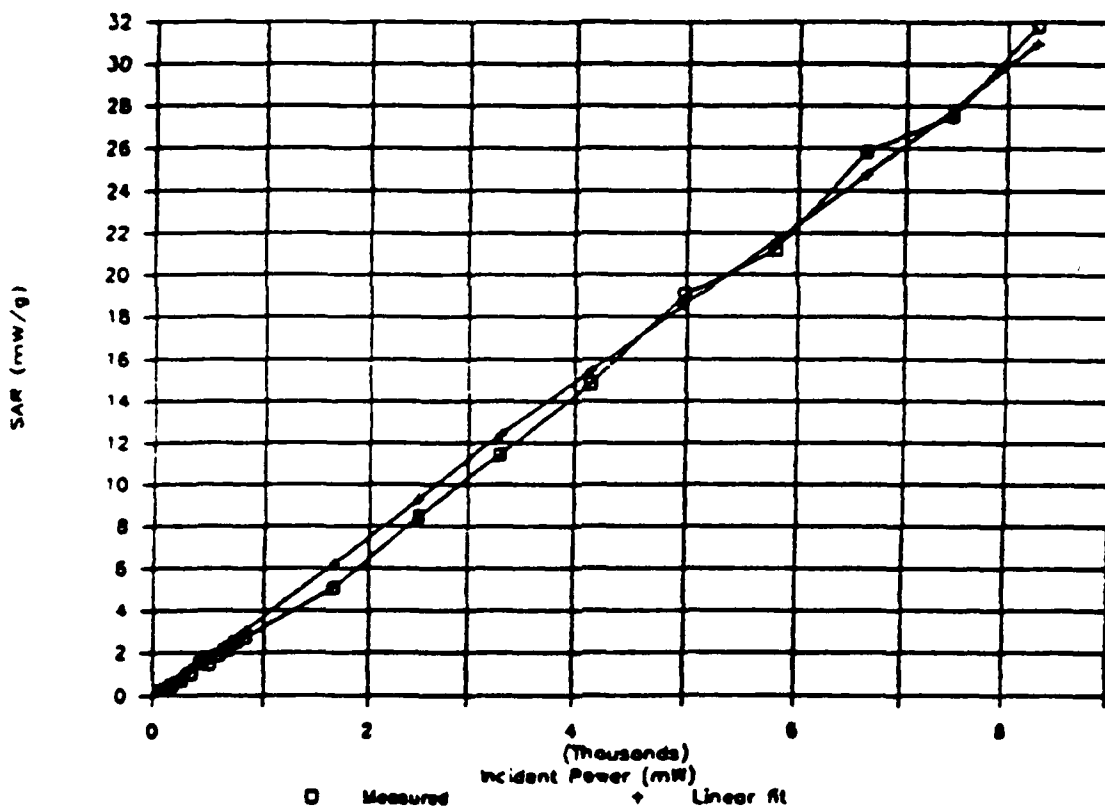## SAR vs.Pinc,4-25cm² flasks č 5 ml medium

Fig. 5: SAR (mW/g) vs. Incident power (mW) for Crawford Cell.

55

Temperature control was provided by a National water jacketed double door incubator. Temperature stability within this incubator is within ± 0.1°C, as measured with a Luxtron fiber optic thermometer. In order to insure that a stable temperature has been reached, samples must be loaded in the Crawford cell at the same temperature as the incubator temperature (experimental temperature) and allowed to equilibrate for at least one hour prior to irradiation.

Additional temperature measurements were carried out to determine the operating SAR range within which no additional temperature control is needed to maintain temperature stability. The results of these measurements are shown in Table II. These results indicate that under the described conditions the system can be operated at SAR's below about 5 mW/g without inducing an appreciable temperature increase within the sample.

TABLE II. Temperature increase at various SAR levels.

SAR	Equil temp	Temp increase
		in 10 mins.
(mW/g)	(°C)	(°C)
4.7	38.65	0.05
8.3	38.7	0.30
27.5	41.3	1.20

E.   Test fixtures for measurements of dielectric response.

Measurements of the dielectric response of essential compounds present within a biological cell such as DNA and other polynucleotides, offer a means to gaining some understanding of the basis of the interaction of electromagnetic fields with biological matter.

Two test fixtures have been designed to perform these measurements, one for frequencies below 40 MHz and the other one for frequencies above 45 MHz. A Hewlett Packard 4194A Impedance/Gain Phase Analyzer was used for measurements in the range between 100 Hz and 40 MHz. A major problem for measurements at lower frequencies is electrode polarization, particularly when measuring conducting samples. This effect can sometimes be present even at the low MHz range. This problem can be corrected for by using movable electrodes. Bearing this in mind, a Hewlett Packard 16451A dielectric cell with movable electrodes and specially modified to accept liquid samples was selected to make the low frequency measurements. Initial measurements, however, have shown that additional steps are necessary to overcome the electrode polarization effect. A commonly used procedure is to coat the electrode

56

surfaces with platinum black. While this cell may be adequate once the electrode surfaces are properly treated, it requires a relatively large sample. A separate cell will be built for smaller samples based on a design by Dr. Kenneth Foster (private communication).

Beyond a few hundred MHz dielectric measurements can no longer be made with the impedance bridge technique. A viable approach is the use of coaxial lines which can generally be used between 40 MHz and 18 GHz. This technique makes use of the reflected signal from a sample located at a defined reference plane along the coaxial line. A wide range of sample configurations are possible. In all cases the sample is placed at the end of a coaxial line of characteristic impedance Z_0. The sample may constitute part of the coaxial line or be placed or be placed at the end of the line. The latter case is that of an open ended coaxial line. For our purposes, a dielectric cell was designed based on a GR-900 connector. The connector design was modified such that the teflon support for the inner conductor extended past the end of this conductor forming a cup to hold the sample. The outer conductor which was flush with the end of the teflon support was shorted with a cap thus closing the cup to seal the sample and complete the circuit. A filling chamber connected by two small holes with the sample chamber was built in the shorting cap and sealed with a rubber septum. This allows loading of the sample chamber after creating a vacuum to eliminate air bubbles. Measurements with this cell were conducted with a Hewlett Packard 8510 Network Analyzer. Initial results indicated that the practical useful range is below 1.5 GHz. An open ended coaxial line will be used to probe the dielectric response at frequencies above 1 GHz.

57

II. BIOLOGICAL APPROACH TO THE PROBLEM

Our initial research efforts on effects of microwave irradiation on cultured cells involved a toxicological, or "cell injury" approach. This approach was based on the idea that events such as DNA synthesis in S phase, mitosis, and survival following plating at low density are dependent on a complex assemblage of metabolic events, and that perturbation of any component event would thus affect the observed end point. These efforts were emphasized in Year 1, and are summarized in that annual report. Additional examinations of related endpoints, using proliferating suspension-adapted cells, HL60 cells and a transport epithelium cell line are summarized in this report. Perturbations of cell proliferation, plating efficiency or viability were not found after microwave exposure. Examination of cell cycle timing and of membrane-related differentiation functions also showed no effects of microwave exposure. These observations represent a clarification of a confusing situation in the literature, where microwave effects have been reported, but without adequate distinction between thermal and athermal conditions. Given the data accumulated to date, it would seem that athermal effects of microwave irradiation are probably subtle, and best approached at the molecular level.

Two specific enzyme systems were selected for analysis during year 2. The rationale for selecting these systems is detailed below. Additionally, a high resolution, two dimensional gel electrophoresis system was developed to allow examination of synthesis of many polypeptides. The selected enzymes and the electrophoresis systems are complementary, in that both specific endpoints and general endpoints are being approached on the molecular level.

1. Use of Proliferating Suspension Cultures, and Crawford Cell Exposures

Previous experiments were done using cells which had been released from their growth surface, placed temporarily into suspension for irradiation, and then returned to monolayer growth for subsequent assay. These cells, which had not been adapted to permanent suspension culture, were not actively proliferating during the temporary suspension conditions employed for microwave exposure. In order to obtain cells that would actively proliferate in suspension conditions, L929 monolayer cultures were placed at high density into spinner flasks with low calcium medium, and cell density was allowed to decrease as adaptation occurred, and active growth was observed.

Suspension-adapted L929 cultures were exposed to conditions previously used for irradiation of temporarily suspended cells. These included exposures to 300 mW/g average SAR microwaves at 37°C, as well as exposures at temperatures of 39, 41 and 42°C. In no case was any differential effect observed in cell proliferation, plating efficiency or viability as the result of microwave exposures. Actively proliferating cells thus were not more susceptible to microwave effects than cells temporarily suspended.

Installation of the Crawford Cell by Engineering provided needed facilities for irradiation of proliferating monolayer cultures. The previously used wave guide devices provided sufficient space for use of suspension cultures, or of small coverslip monolayer cultures. The coverslip cultures provided too few cells for adequate analysis by biochemical or flow cytometry techniques. Availability of the Crawford cell allowed exposures at 0.9 GHz and with cell quantities sufficient for biochemistry and cytometry.

Initial exposures were conducted at 5 mW/g SAR to confirm results previously obtained with suspension cultures at 2.45 GHz conditions. Exposures at this SAR yielded a 15% increase in cell number of microwave over control cultures after 72 hrs. As a consequence of these observations the engineering group made measurements, and determined that slight elevation of temperature (less than $0.5°^{(C)}$ was occurring at 5 SAR. Subsequent exposures at SAR of 1 mW/g were done, conditions under which no heating was measured, and showed no increase in cell number of exposed over control samples. Installation of a fan in the incubator minimized temperature buildup within the Crawford cell due to microwave absorption, but any subsequent long term exposures (greater than approx. 4 hrs.) were conducted at SARs of 3 mW/g or less to avoid heating artifacts.

2. Cell Cycle Analysis

Methods

Cultures of the HL60 cell line were inoculated at 1×10^5 cells/mL and samples were taken for counts of cell density and cell cycle analysis at intervals of twenty-four hrs. These samples provided baseline information needed for accurate setup of log phase cultures for irradiation experiments. Typical DNA profiles of log phase cultures are represented by the non-irradiated samples as shown in Fig. 1 and Table 1. Results from this work indicated that cultures established 24 hr. prior to irradiation would double in cell density, to 2×10^5 cells/mL, by the time of irradiation and be in log phase growth during the course of the experiment.

Cells to be analyzed by flow cytometry were processed for propidium iodide DNA staining according to the methods outlined in Protocol # 27, from Ortho Diagnostics. This protocol, which

59

involves lysis of the cell with non-ionic detergent, was selected since it allowed immediate processing of cells without the need for extended, RNase digestion, and since it minimized cell clumping. DNA content was analyzed for 10,000 cells per sample using an Ortho Cytofluorograf. Each sample was analyzed in quadruplicate for sham and irradiated cultures, and in duplicate for non-irradiated controls. On the basis of the DNA profile, regions were selected to represent G1, S and G2/M phases of the cell cycle, and the percent of total cells in each stage was calculated.

Irradiation conditions consisted of 0.9 GHz microwaves which were modulated (80%) at 60, 400 or 1,000 Hz, with an SAR of 2 mW/g. These irradiations were done for 24 hr. in a Crawford cell, with cells maintained in sealed, 25 cm^2 flasks. Sham irradiated cells were placed outside the Crawford cell on a shelf in the incubator, and non-irradiated controls were maintained in the CO_2 incubator in which the cells were grown prior to the experiment.

Results

Typical DNA profiles for non-irradiated, sham and microwave irradiated samples are shown in Fig. 1. Profiles were remarkably consistent from experiment to experiment, and within experiments. Table 1 compares the cell cycle distributions obtained for the three irradiation conditions applied. In no case was there a significant difference within an experiment to indicate an alteration of cell cycle progression due to microwave irradiation. Variation for a given cell cycle stage between sham and irradiated samples was within 1% for all experiments, and these samples displayed no stage specific variation of more than 2.0% compared to the non-irradiated controls which were maintained in a separate incubator. Cell cycle distribution was thus unaffected by microwave exposure over a 24 hr. interval. Cell viabilities and densities, determined at the end of each experiment, were comparable among all three samples for each experiment.

60

Table 1: Cell Cycle Distributions After Microwave Irradiation

Modulation	Sample	% Cells In		
		G1	S	G2/M
60 Hz	NE	11.6	8.6	79.8
	SH	11.8 ±0.9	8.4 ±0.3	79.4 ±1.1
	MW	12.2 ±0.4	8.4 ±0.8	79.4 ±1.1
400 Hz	NE	21.3	12.6	66.1
	SH	19.6 ±0.4	10.7 ±0.2	69.7 ±0.4
	MW	19.7 ±0.9	10.9 ±0.5	69.4 ±1.0
1000 Hz	NE	18.8	7.4	73.8
	SH	18.5 ±0.7	7.1 ±0.2	74.4 ±0.7
	MW	17.7 ±0.8	7.1 ±0.1	75.2 ±0.8

NE = nonexposed control, SH = sham exposed, MW = microwave exposed

3. Cell Differentiation Experiments

Porcine cells of the LLC-PK line represent one of several established mammalian cultures which exhibit differentiated characteristics of a transport epithelium when grown to confluency (11). Confluent monolayers establish apical tight junctions between adjacent cells, and transport water passively across the monolayer as the result of active transport of salts and sugars. Accumulation of water beneath the monolayer produces a build up of positive hydrostatic pressure, which manifests itself as a loosening of local areas of the monolayer from the growth surface. This produces transient "blisters" or "domes" in which areas of the monolayer elevate, and subsequently lower back onto the growth surface, presumably as hydrostatic pressure ebbs with leakage of water through the monolayer. The domes can be counted under the microscope, and the number of domes per microscope field used to quantify the extent of transport activity at a given time. This situation thus allows for microscopic assessment of a complex set of coordinated, differentiated functions. Agents, such as the adenosine analog theophylline, which interfere with membrane transport activity, thus diminish the extent of dome formation (9).

The transport phenomena exhibited by LLC-PK cultures are primarily the result of membrane mediated functions. Since at least some alterations of membrane transport have been associated with microwave exposure (10), it was felt that the epithelial culture system would provide a means of assaying for altered membrane functions.

Methods: LLC-PK cells were maintained as monolayer cultures in Eagle's Minimum Essential Medium supplemented with 10% fetal bovine serum and 20 mM HEPES buffer. Stock cultures were routinely split prior to confluency, so as to avoid problems of diminished cell growth rate following differentiation. For irradiation

experiments cell suspensions were seeded at 1×10^6 cells per dish, into petri dishes coverslips. Coverslips were harvested for experiments after 1 or 2 days growth, depending upon whether confluent or subconfluent specimens were desired. Irradiations were conducted for 24 hr. using either continuous wave conditions at 300 mW/g average SAR, or 1 μsec duration pulses, at 100 pulses per second, at an SAR of 25 mW/g. Irradiations were conducted in the temperature control device previously described, with sham samples held in an identical device but without microwave exposure. Control cultures, maintained in the original incubator, were assayed for dome formation prior to, and immediately after, each experiment. Dome formation was assessed by fixing coverslip preparations in 2% glutaraldehyde in phosphate buffered saline to preserve the dome conditions immediately at the end of exposure, and then counting domes per field, using phase contrast optics, for an area of 40 mm^2. Variation in the number of domes per area was found between different platings of cells, but was consistent within an experiment. To assess the ability of the cells to show response to perturbations by altering dome formation, some cultures were treated with 0.1 mM theophylline.

Results: Application of theophylline to confluent LLC-PK cultures reduced dome formation by 40%, with control populations showing an average of 45 domes per field, and theophylline treated cells 27 domes per field.

Irradiation experiments were conducted of both confluent and subconfluent cultures, with the idea that irradiation might interfere with either establishment of, or maintenance of, a transport epithelium. In none of the experiments conducted, with either continuous or pulse wave exposures, was a significant difference in dome formation observed. Representative values are given below for two exposures.

Table 2: Dome Analysis of LLCPK Cultures

Confluent Culture, Pulsed Wave

Average Domes/Field After Exposure

Sham	18
Exposed	20
Pre-Control	29
Post-Control	22

62

<u>Subconfluent Culture, Pulsed Wave</u>

<u>Average Domes/Field After Exposure</u>

Sham   12

Exposed   11

Post-Control   22

Cultures maintained in the original incubator consistently showed more domes/field than those transferred to the sham or irradiation chambers. This was not due to failure of cells to grow under experimental conditions since subconfluent cultures reached confluency in the irradiation chambers, and initiated dome formation. The constant flow of medium across the coverslips in the chambers and different conditions for gas exchange may explain the difference, as may the transferring of cultures required for insertion in the chambers. Standard deviation for control cultures ranged from ±3-6 domes per field. In no case was the difference in dome density between sham and microwave exposed samples sufficient to indicate an effect.

4. **Enzyme Activities and Microwave Exposures**

Ornithine decarboxylase (ODC), an enzyme involved in the production of the polyamines putrescine and spermidine, has attracted considerable research attention (12). ODC is one of the most highly inducible and regulated eucaryotic enzymes, and is involved in pathways important to RNA, DNA and protein synthesis. ODC activity has been shown to vary in response to cell transformation, and correspondingly, increases with cell growth and proliferation. Given the possibility of alterations in membrane electrical activity by exposure to electromagnetic fields, and the fact that ODC activity responds to stimuli via membrane-mediated second messengers, it has been selected as a subject for investigations of electromagnetic field effects. Two to five fold elevations in ODC specific activity have been reported for mammalian cultures exposed to 60 HZ electromagnetic fields, 10 mV/cm for 1 hr (1). Increased activity has also been reported for exposure of cultures to 450 MHz microwave irradiation modulated at 10-20 Hz (2).

We selected ODC as an enzyme for investigation since it has been demonstrated to respond to electromagnetic effects, and due to its involvement in several essential biochemical pathways.

Additional enzymes were selected for investigation which had not been previously examined for responses to electromagnetic fields, but whose importance to the functioning of the immune system, and whose regulation via membrane receptors, suggested

63

fruitful possibilities for investigation. The enzymes selected, 2',5'-oligoadenylate synthetase (2-5A synthetase), and the 2-5A-dependent RNase (RNase L) are synthesized by cells following response to interferon. Upon interferon stimulation, basal level activities are elevated from three to several thousand fold for 2-5-A synthetase and up to 30 fold for RNase L, depending upon the cell line and other factors (15). Elevation in 2-5A synthetase activity results in synthesis of 2' to 5' linked oligoadenylates from ATP. This 2-5A activates RNase L, which cleaves cellular or viral single-stranded RNA at sites following UU or UA sequences. Approximately 24 hrs post stimulation is required for maximal activity of either enzyme to be realized after exposure to interferon. The two enzymes have been implicated in the anti-viral and growth inhibition effects of interferon, and may also be involved in cellular differentiation and growth regulation (7).

ODC Assays

Methods: Stock cultures of L929 cells were grown as monolayers in Eagle's Minimum Essential Medium supplemented with 10% fetal bovine serum and 20 mM HEPES buffer. 3.5 mL of cell suspension, $2x10^6$ cells/mL, from midlog phase cultures were used for each sham or microwave irradiation. Microwave and sham exposures were carried out at 300 mW/g average SAR, 37°C, for 4 hr in the wave guide apparatus already described. Cells were then harvested for assay. Cells were harvested directly from monolayer for the "culture phase" ODC assay.

ODC Specific Activity Measurements: Cells were washed 3 times in cold PBS and then frozen at -70° C for storage. Thawed pellets were suspended in lysis buffer (25mM Tris, pH 7.5, 2.5 mM dithiothreitol, 0.1 mM EDTA, 0.1% Nonidet P-40), and S-10 fractions prepared by centrifugation at 10,000 rpm for 15 min, 4°C. Protein determinations were done by use of the Bio-Rad commassie blue method. 100 μg of S-10 sample protein was used in a 250 μL assay mixture including 40 μM L-ornithine, 275,000 dpm L-[^{14}C]-ornithine (approx. 50 mCi/mMole), 4 μM pyridoxal phosphate, 1.25 mM dithiothreitol and 5.0 mM Tris-HCL, pH 7.5. The reaction was carried out by incubation, 37°C, in stoppered test tubes carrying polypropylene wells containing 200 μL, 1M hyamine hydroxide. After 60 min the reaction was stopped by injection of 300 μL 20% TCA through the rubber stopper. Acid-released $^{14}CO_2$ was dissolved in the hyamine hydroxide during a further 30 min incubation at 37°C. The well containing the hyamine hydroxide was removed, the hydroxide neutralized with 5 μL glacial acetic acid, and the well placed into a scintillation vile for counting (13).

Results: ODC activities have been shown to vary with the state of cell proliferation. To assure consistent conditions for microwave experiments cultures were established and allowed to progress, over five days, through initial lag phase, into log phase growth and into stationary phase. ODC activities were measured at

64

0 and 4 hrs. and then at 24 intervals. Results are presented in Table 3. These data provided baseline ODC values for L929 cultures, and demonstrated that ODC regulation was occurring. Subsequent cultures for irradiation were accordingly allowed to progress to late log phase for use, so as to provide cells for exposure that exhibited baseline levels of ODC, but which were actively proliferating.

Also, to be sure that alterations in ODC activities by exogenous agents would occur with the L929 cell line, cultures were exposed to phorbol methyl ester in concentrations ranging from 160 to 1280 nM. Regulation was observed, with the 640 nM yielding approximately 3 times higher ODC activity than comparable controls.

Table 3: Variation in ODC Activities with Culture Conditions

Time (hrs)	Phase of Growth	ODC Activity (units/g protein)
0	Inoculum (Late Log Phase)	3.9 ± 1.6
4	Lag Phase	122 ± 10.0
24	Early Log Phase	60.6 ± 9.7
48	Mid Log Phase	13.3 ± 5.7
72	Late Log Phase	3.7 ± 1.0
96	Early Stationary Phase	3.1 ± 1.1
120	Late Stationary Phase	0.6 ± 0.6

One unit equals the amount of enzyme releasing 1 nanomole of $^{14}CO_2$ per minute at 37°C.

Results from ODC assays of 3 preliminary experiments involving 4 hr sham or microwave exposures at 300 mW/g SAR were initially compiled. Specific activities of microwaved samples were virtually identical to those of sham irradiated samples, with values of 56 ± 17, and 54 ±18 units/g protein, respectively. As follow up to these data a series of exposures of L929 monolayers was begun, using the Crawford cell and SARs of 3-5 mW/g, over a time course of 0 to 8 hrs. Additional experiments were begun using the human cell line HL60, and repeating the four hour exposures in suspension, using continuous wave or pulsed microwaves. These experimental series were initiated at the end of the grant year.

B. Interferon System

Methods: Mid log phase L929 monolayer cultures, grown in 150 cm² flasks, were trypsinized and placed into suspension at a density of 5x10⁶ cells/ML. Cells for microwave or sham exposures were placed into 3.6 mL tubes, inserted into the temperature controlled waveguide devices previously described, and maintained in suspension with stirring during the period of irradiation. Monolayer cultures, maintained in the original incubator, were retained for subsequent basal level control values, or were treated

with interferon (100 IU murine alpha plus beta) for positive controls. Irradiations were at 300 mW/g average SAR, 2.45 GHz, for 4 hours at 37°C. Following irradiation cells were returned to tissue culture flasks and incubated at 37°C for 18 hr. In other experiments cells were maintained as log phase monolayers in 25 cm^2 flasks, and irradiated at 5 mW/g SAR in the Crawford cell for 4 hr, and incubated an additional 18 hr. Cells were then harvested, washed in cold PBS and pellets frozen at -70°C. Pellets were lysed and S-10 fractions prepared as in the ODC assay.

2-5A synthetase activity was assayed by isolating 2-5A synthetase from S-10 fractions onto poly(I)-poly(C)-cellulose, followed by incubation with 4.0 mM ATP for 2 hr at 37°C (17). 2-5A synthesis was measured by direct competition radiobinding assay using [^{32}P]-2,5A (6). Units of synthesis were nMoles of 2-5A synthesized/mg protein/hr.

RNase L activity levels were monitored by binding of [^{32}P]-2,5A. 100 μG S-10 protein was incubated with 5,000 cpm [32 P]-2,5A overnight at 0°C (6). Samples were filtered through nitrocellulose and binding measured by scintillation counting of filter-bound radioactivity. In order to measure RNase L specific activity the enzyme was immobilized and partially purified from S-10 preparations using 2-5A bound to cellulose. The degradation of poly(U)-[^{32}P]Cp (10,000 cpm/time point per specimen) was assayed in the presence and absence of 100 nM trimer 2-5A as a means of demonstrating enzyme specific activity. 20 μL aliquots were precipitated, and results expressed as percent of original cpm remaining for each time point (14).

Results: Comparison of 2-5A synthetase specific activities from microwaved and sham populations of suspension cells and from control monolayer cultures revealed no significant changes in enzyme activity as either a result of microwave exposure, or of cell handling conditions (Fig. 3). Interferon treated monolayers, however, exhibited an anticipated increase (approx. 191 fold) in 2-5A synthetase activity from 163 to 31,200 units.

Binding of 2-5A by RNase L was affected both by conditions of cell handling, and by microwave exposure. This is demonstrated in Fig. 4. Expressed as a percent of control binding, the sham-irradiated cells showed an approximately 19% increase, microwave irradiated cells an approximately 42% increase and interferon-treated monolayers approx. a 67% increase in binding. Removal of cells from the growth surface and maintenance under sham conditions for 4 hrs thus produced an increase in RNase L binding activity. Addition of microwave exposure more than doubled this binding activity, but did not reach the levels achieved when interferon was added to monolayer cultures subjected to neither sham nor microwave conditions.

Increased RNase L activity in response to microwave exposure

was further investigated by measuring RNase L specific activity to assess whether increased binding actually indicated increased enzyme catalytic activity. Results of these measurements are presented in Fig. 5. Results paralleled those for 2-5A binding, with highest activity displayed by interferon treated monolayer controls, lowest activity by non-treated monolayers, and sham and microwave irradiated samples showing respective increases over non-treated monolayers. This established the fact that the more readily performed 2-5A binding assay for RNase L could be used as an indicator of increased enzyme specific activity.

These results were of particular interest due to the fact that only one of the two enzymes, RNase L, displayed increased activity in response to microwave exposure. Under conditions of interferon stimulation both enzymes would show increased activity. The increased RNase L activity of the sham-irradiated cells may have resulted from their removal from monolayer and 4 hr. of suspension culture, during which time no cell proliferation would be expected to occur. RNase L activities may be altered if cells are maintained in non-proliferating conditions (5,8). Given these facts it was decided to irradiate cells maintained in monolayer culture. Irradiations for 4 hrs at 5 mW/g SAR were conducted in the Crawford cell and RNase L binding activities were measured after 18 hr additional incubation. Results from six experiments are compiled in Table 4. As can be seen from the table the results obtained were equivocal. Average values were slightly higher for the microwaved samples, but sample to sample variation was high, giving standard deviations too large for any conclusions to be drawn. Lower than anticipated protein values for the S-10 samples of the least 3 experiments suggested that at least some of the variation might have stemmed from unanticipated problems with cell cultures or early processing of the cell pellets. At the end of the grant year these experiments were being repeated to minimize sample to sample variation and so determine whether the effect could be duplicated with a proliferating population.

Table 4: RNase L Binding Activities of Irradiated Monolayers

Experiment #	Percent of Control CPM [^{32}P]-2-5A Bound	Mean ±SD
Sham 1	128.0	
2	106.0	
3	71.1	
4	71.1	
5	54.1	
6	60.7	81.8±29
MW 1	137.0	
2	140.0	
3	139.0	
4	57.8	
5	54.1	
6	66.7	99.1±44

67

5. 2-D Gel Electrophoresis

Given the difficulties involved in hypothesizing which cell products would most likely be affected by exposure to microwave or other electromagnetic radiation, a more global approach to examining molecular perturbations of the cell was sought to complement the work on specific enzymes. Two dimensional gel electrophoresis (2DGE) allows high resolution of polypeptides and, combined with isotope labeling techniques, provides a well defined means of analyzing many translation products simultaneously (Cellis and Bravo, 1984).

Facilities and techniques for performing translation assays by 2DGE were established. Using a pH 3-10 gradient for the isoelectric focusing first dimension, and 10% polyacrylamide SDS slab gels for the second dimension, a system was established capable of resolving approximately 1100 different HL60 polypeptides when used in conjunction with silver staining. Labeling of cells with ^{35}S-methionine at 20-30 μCi per $3x10^6$ cells in methionine free medium provided sufficient specific activity in 30 to 60 min to load $5x10^5$ cpm or more per gel. This activity allowed exposures of 2 to 4 days for adequately resolving approximately 600 polypeptides on X ray film, provided gels were impregnated with a water soluble fluor before drying.

Initial experiments involving exposure to microwaves were done while the conditions for labeling and fluorography were being developed. HL60 cells grown in 25 cm^2 flasks were used as controls or exposed samples for SAR 3 mW/g continuous wave or 60 Hz sine wave modulated, 0.9 GHz microwaves for 24 hr. Proteins were stained with silver, and control and experimental pairs were examined manually to see if spot patterns of the polypeptides had changed. No significant changes were found in these samples, but since the silver technique stains all proteins, and is not selective for those synthesized during exposure, only very pronounced alterations in synthesis might be detected. For example, the new appearance of a large quantity of one or a few polypeptides would be readily observed. Variations in synthesis over shorter time intervals might also not be detected. Subsequent exposures, initiated at the beginning of year 3 have employed isotopic labeling and fluorography, so that only the polypeptides synthesized during exposure will appear.

6. Discussion

Results from Year 2 verified that microwave exposed actively proliferating cells displayed the same resistance to perturbations of cell growth, viability and plating efficiency, and the same thermal susceptibilities, that were seen with monolayer cultures temporarily suspended for irradiation. Further, membrane related

differentiation functions of the cell line LLC-PK were not altered by either continuous wave or pulses microwave exposures over periods of 24 hr.

Crawford Cell irradiations of actively proliferating cultures of the HL60 cell line showed no alterations of cell cycle distribution between sham irradiated specimens and those exposed to either continuous wave or modulated microwaves at 0.9 GHz. These results resolve the earlier question as to whether cell cycle shifts were observed in cultures which subsequently displayed very low level bacterial contamination. Healthy, actively growing cells were not altered in cell cycle progression by 24 hr. of microwave exposure.

Of the two enzyme systems selected for analysis one, the interferon related system, showed response to microwave exposure. RNase L binding and 2-5A activities showed an approximate doubling over sham values, and approx. 40% increase overall when compared to monolayer controls. The sham values (20% over controls) may result from cessation of cell proliferation during the 4 hr irradiation period. The question that arises under these circumstances is whether microwave irradiation is influencing RNase L gene regulation in some direct way, or is affecting it indirectly through some effect related to cell proliferation. None the less, it is interesting that the effect observed was approx. two thirds that seen in interferon treated monolayers, and that the RNase L increase was not concomitant with a corresponding increase in 2-5A synthetase activity. Additional exposures of monolayer cultures at 0.9 GHz will be conducted in year 2 to see if irradiation of actively proliferating monolayer cells will produce the same results, a possibility suggested by the initial data reported here. Additional assays will be done for the HL60 human cell line.

The regulation of ODC activity in L929 cultures was established, and the information used to initiate assays of microwave exposed samples. Initial results showed no significant alterations as the result of microwave irradiation, but this work will be continued to explore a number of exposure conditions, and to investigate results in both the L929 and HL60 cell lines. The regulatory flexibility of ODC (12) makes it an attractive candidate target for electromagnetic exposures, and will be further pursued.

The two dimensional gel electrophoresis system yielded no detectable differences in protein patterns when silver staining was used to compare sham and exposed cultures. Only gross perturbations would likely have been detected under these circumstances, however, and isotopic labeling was required for more sensitive assay. Labeling and fluorographic conditions using S-35 methionine have been established, allowing up to 1×10^6 cpm to be loaded onto each gel for detection of even small amounts of proteins. Experiments were begun to analyze isotopically labeled proteins, examining results initially from ELF exposures at 60 Hz,

and then progressing into modulated microwave exposures.

   With the desire to extend analysis further into the molecular realm, experiments were planned for Year 3 to examine general RNA alteration as well as specific mRNA variation due to ELF and to microwave exposures. The experiments planned, as well as extensions of those already in progress, would thus cover general and specific transcriptional patterns, general translational patterns, and specific enzyme activities.
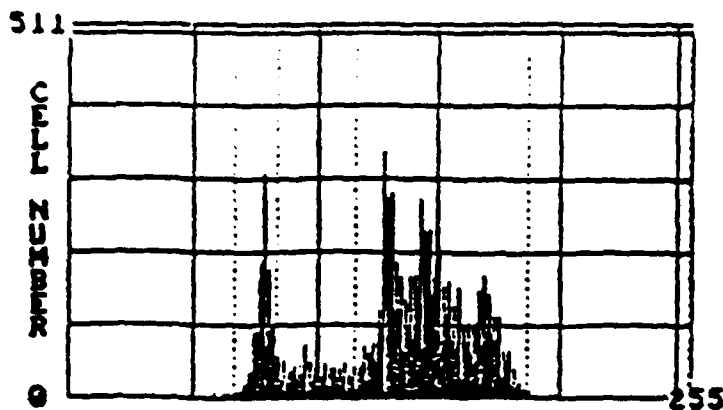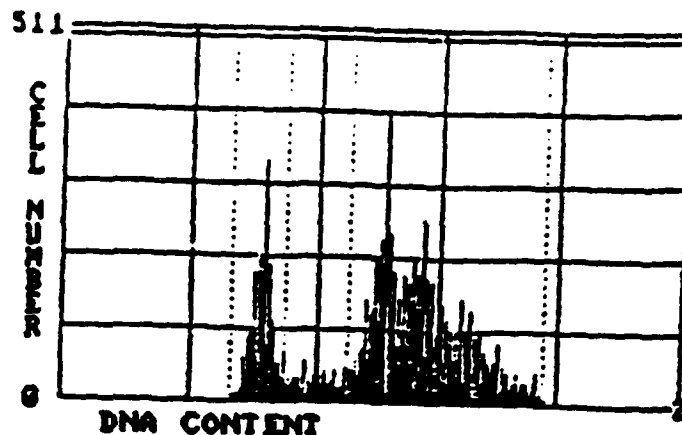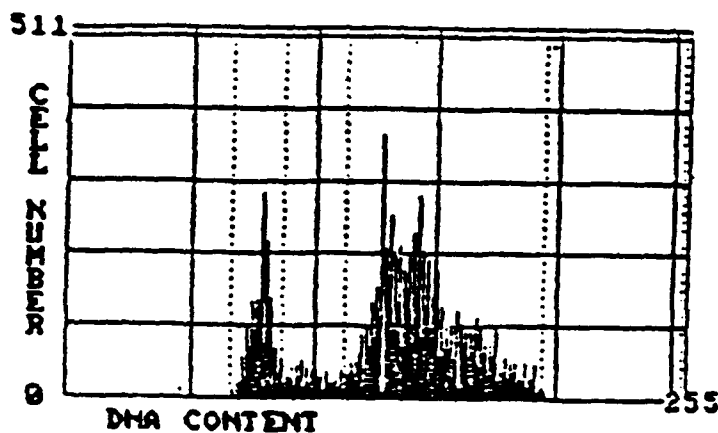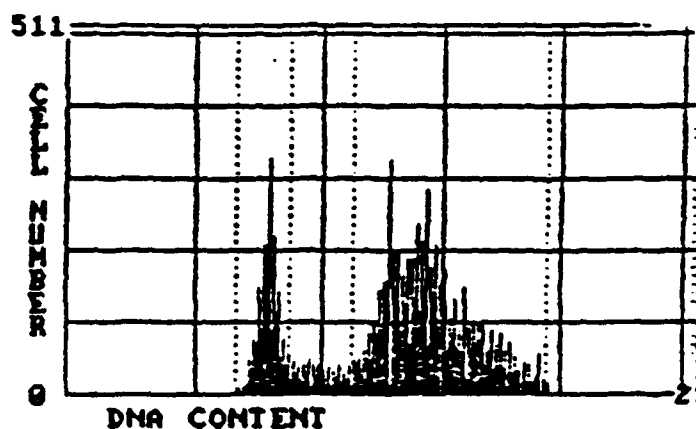
Figure 1a

Figure 1b

Figure 1c

Figure 1d

Figure 1: DNA distributions for log phase HL60 cultures, as determined by flow cytometry. The Y axis is cell number for a given level of DNA fluorescence, and the X axis the relative amount of DNA as determined by propidium ioidide fluorescence. Dotted vertical lines indicate the approximate divisions for G1, S and G2/M amounts of DNA. 1a. Controls, pre-irradiation; 1b. Controls, post-irradiation; 1c. Sham irradiated; 1d. Microwave exposed, 0.9 GHz, 400 Hz, 80% modulation, 24 hr.
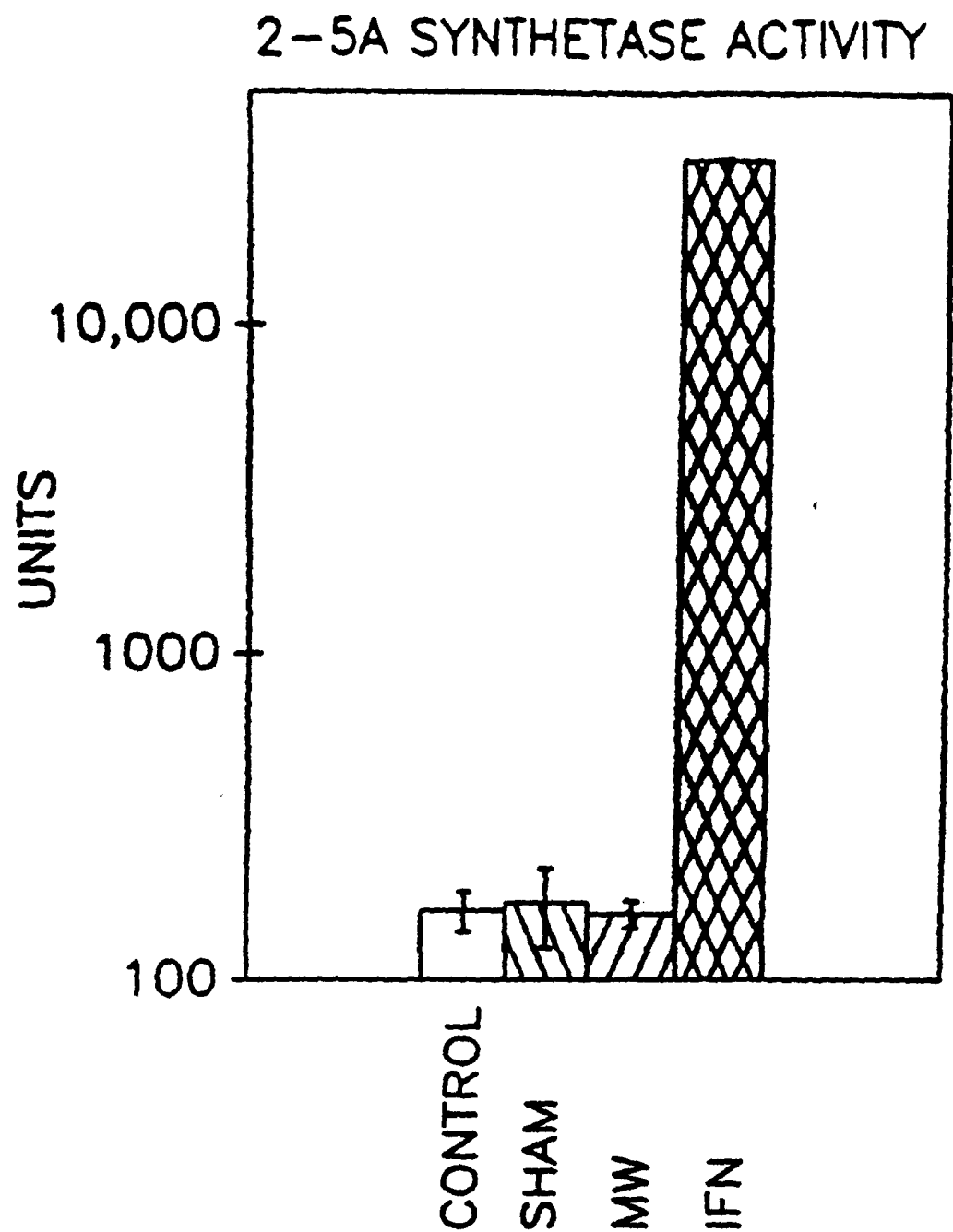
2-5A SYNTHETASE ACTIVITY

Figure 2. 2-5A Synthesis Activities at 37°C. Units are nanomoles of 2-5A synthesized per mg protein per hour.

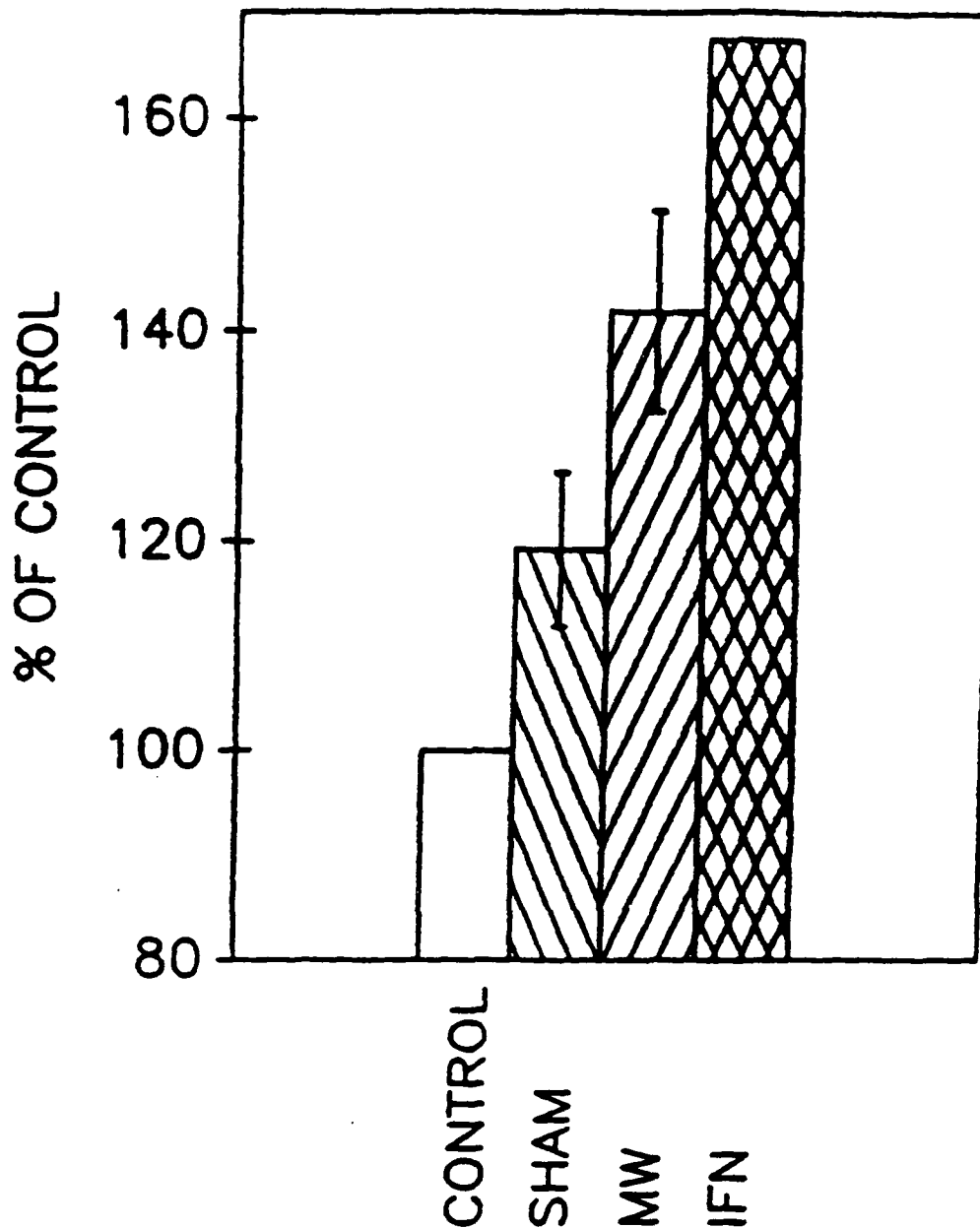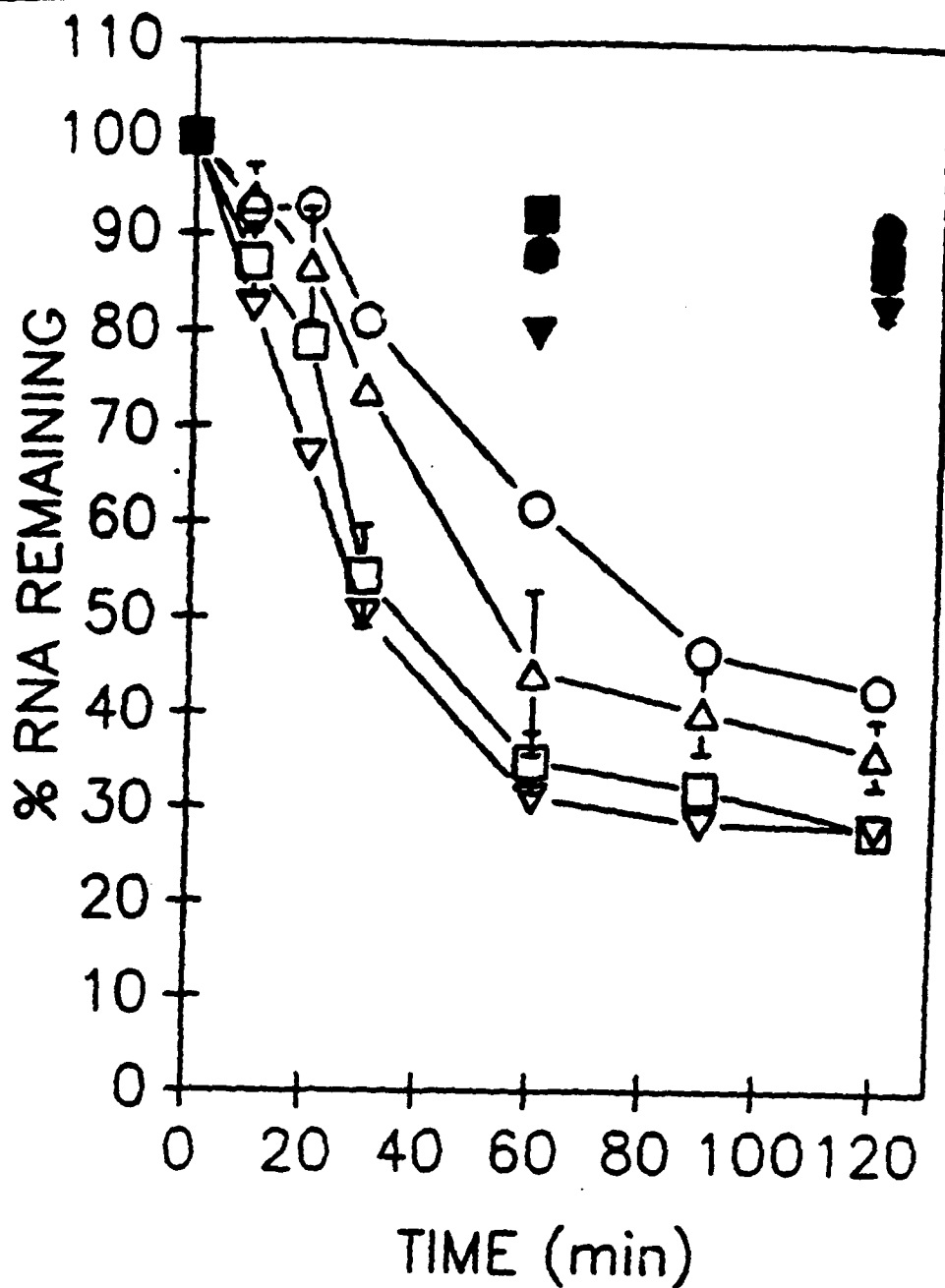Figure 3. Binding of ^{32}P labeled 2-5A. Values are given as percent of binding by control monolayer cells.

Figure 4. Degradation of Poly (U)-[^{32}P]Cp by RNase L. Symbol designations are as follows: circles = monolayer control; upright triangles = sham irradiated; squares = microwave-irradiated; and inverted triangles = interferon-treated monolayers. Closed symbols represent assays done in the presence of unlabeled trimer 2-5A (100 nM); open symbols represent assays done without 2-5A.

74

References

1. Byus, C.V., Pieper, S.E. and Adey, W.R. <u>Carcinogenesis</u>, 8:1385-1389, 1987.

2. Byus, C.V., Kartun, K., Pieper, S.E. and Ady, W.R. <u>Cancer Res.</u>, 48:4222-4226, 1988.

3. Cellis, J.E. and Bravo, R. (Eds) <u>Two-Dimensional Gel Electrophoresis of Proteins</u>, New York, Academic Press, 1984.

4. Jacobsen, H., et al. <u>Virology</u>, 125:496-501, 1983.

5. Jacobsen, H. et al. <u>Proc. Natl Acad. Sci., USA</u>, 80: 4954-4958, 1983.

6. Knight, M., et al. <u>Nature</u>, 288: 189-192, 1980.

7. Krause, D. et al. <u>Eur. J. Biochem.</u>, 146:611-618, 1985.

8. Krause. D. et al. <u>J. Biol. Chem.</u>, 260: 9501-9507, 1985.

9. Lever, J.E. in M. Taub (Ed) <u>Tissue Culture of Epithelial Cells</u>, New York, Plenum Press, 1985.

10. Liburdy, R.P and Vanek, P.F. <u>Radiation Res.</u>, 103: 266-275, 1987.

11. Mullin, J.M. and Kleinzeller, A. in M. Taub (Ed) <u>Tissue Culture of Epithelial Cells</u>, New York, Plenum Press, 1985.

12. Pegg, A.E. and Williams-Ashman, H.G. In D.R. Morris and L.J. Marton (Eds). <u>Polyamines in biology and Medicine</u>, pp. 3-42. New York: Marcel.

13. Seeley, J.E. and Pegg, A.E. <u>Methods in Enzymology</u>, 94:158-161, 1983.

14. Silverman, R.H. <u>Anal Biochem.</u>, 144: 450-460, 1985.

15. Silverman, R.H., et al. <u>Eur. J. Biochem.</u>, 124: 131-138, 1982.

16. Silverman, R.H., et al. In, E.DeMaeyer and H. Schellickens (Eds) <u>The Biology of the Interferon System 1983</u>, pp. 189-200, 1983.

17. Stark, G.R., Brown, R.E. and Kerr, I.M. <u>Methods in Enzymology</u>, 79B: 194-199, 1981.